

**DOKUZ EYLÜL UNIVERSITY**  
**GRADUATE SCHOOL OF NATURAL AND APPLIED SCIENCES**

**EXPERIMENTAL INVESTIGATION ON  
THERMAL PERFORMANCE OF Ag–WATER  
NANOFLUIDS**

**by**

**Halil Doğacan KOCA**

**August, 2016**

**İZMİR**

**EXPERIMENTAL INVESTIGATION ON  
THERMAL PERFORMANCE OF Ag–WATER  
NANOFLUIDS**

**A Thesis Submitted to the  
Graduate School of Natural and Applied Sciences of Dokuz Eylül University In  
Partial Fulfillment of the Requirements for Degree of Master of Science in  
Mechanical Engineering Department, Energy Program**

**by**

**Halil Doğacan KOCA**

**August, 2016**

**İZMİR**

**M.Sc THESIS EXAMINATION RESULT FORM**

We have read the thesis entitled “**EXPERIMENTAL INVESTIGATION ON THERMAL PERFORMANCE OF Ag–WATER NANOFLUIDS**” completed by **HALİL DOĞACAN KOCA** under supervision of **ASSOC. PROF. DR. ALPASLAN TURGUT** and we certify that in our opinion it is fully adequate, in scope and in quality, as a thesis for the degree of Master of Science.



Assoc. Prof. Dr. Alpaslan TURGUT

Supervisor



Asst. Prof. Dr. Mehmet Akif EZAN

(Jury Member)



Asst. Prof. Dr. Ziya Hakstan Karadeniz

(Jury Member)



Prof. Dr. Ayşe OKUR

Director

Graduate School of Natural and Applied Sciences

## ACKNOWLEDGMENTS

I would like to express my special thanks to my supervisor, Assoc. Prof. Dr. Alpaslan TURGUT for his patient supervision, guidance and everlasting support throughout my graduate education. Studying with him was a privilege and helped me to decide to pursue an academic career. I truly appreciate her encouragement and belief in me.

I also would like to thank Asst. Prof. Dr. Mehmet Akif EZAN, Asst. Prof. Dr. Levent ÇETİN and Asst. Prof. Dr. Ziya Haktan KARADENİZ for being my examiner and for the advisable suggestion.

I want to express my sincere gratitude to Res. Asst. Serkan DOĞANAY for helping me at every stage of my academic life. I appreciate his kind and perfectionist attitude, as well as his attention on my experiments.

I wish to express my special thanks to Res. Asst. Tuba EVGİN, Ali MACİT and Alim ZORLUOL for their contributions and great help.

Finally and most importantly, I would show my best thank to my family and my fiancée İpek Merve GÜRSES for their unlimited support in my whole life.

This work has been supported by Research Foundation of Dokuz Eylül University (project no: 2013.KB.FEN.016).

Halil Doğacan KOCA

# EXPERIMENTAL INVESTIGATION ON THERMAL PERFORMANCE OF Ag-WATER NANOFLUIDS

## ABSTRACT

The goal of the present study is to investigate experimentally the thermal conductivity and viscosity of silver-water nanofluid and its thermal performance in a single-phase natural circulation mini loop.

The experiments were performed both with silver-water nanofluids and de-ionized water. The silver-water nanofluid with 5 percent (in weight) concentration, which contains polyvinylpyrrolidone with 1.25 percent (in weight), was purchased. This sample was diluted with de-ionized water to four different concentrations of 0.25, 0.5, 0.75 and 1 percent (in weight). Thermal conductivity and viscosity of nanofluids were measured by  $3\omega$  method and Brookfield rheometer, respectively. An effectiveness factor was used to define the thermal performance of the mini loop. Throughout the experimental period, operating parameters such as inclination angle and input power to the heater of the loop were varied in the range of 0 to 60° and 10 to 50 Watt, respectively. Moreover, the effect of using polyvinylpyrrolidone on thermal conductivity, viscosity and thermal performance of nanofluids has been discussed and the results were compared with other studies in the literature.

As a result, the experiments showed that current samples were found to be more viscous and thermally less conductive than the values in the literature. However our measurements appear to be more compatible with polyvinylpyrrolidone solution results in the literature. It is concluded that all nanofluid samples have an enhanced effectiveness factor up to 8.6 percent (25 Watt) than the de-ionized water and the effectiveness of the mini loop show an enhancement with increase in inclination angle and particle concentration at all applied power.

**Keywords:** Nanofluid, silver, surfactant, mini loop, thermal performance, thermal conductivity, viscosity, polyvinylpyrrolidone, single phase, natural convection

# Ag-SU NANOAKIŞKANIN ISIL PERFORMANSININ DENEYSEL İNCELENMESİ

## ÖZ

Bu çalışma, gümüş-su nanoakışkanın ısı iletkenliğinin, viskozitesinin ve tek fazlı doğal taşınımlı mini döngüdeki ısı performansının deneysel olarak incelenmesini amaçlamaktadır.

Deneysel de-iyonize su ve gümüş-su nanoakışkanlarla gerçekleştirilmiştir. Kütleli olarak, yüzde 1,25 polivinilpirolidon ve yüzde 5 gümüş tanecikler içeren gümüş-su nanoakışkan temin edilmiş ve dört farklı konsantrasyona (kütleli yüzde 0,25–1) seyreltilmiştir. Nanoakışkanların ısı iletkenliği ve viskozitesi sırasıyla  $3\omega$  yöntemiyle ve Brookfield reometresiyle ölçülmüştür. Sistemin ısı performansının belirlenmesi için ise, sistemde gerçekleşen ısı transferinin mümkün olan en yüksek ısı transfer miktarına oranını temsil eden etkinlik katsayısı kullanılmıştır. Deneysel sırasında, döngünün ısıtıcı gücü ve eğim açısı gibi çalışma parametreleri, sırasıyla 10-50 Watt ve 0-60 derece olarak değiştirilmiştir. Bunlara ek olarak, polivinilpirolidon kullanımının gümüş-su nanoakışkanın ısı iletkenliği, viskozitesi ve termal performansı üzerindeki etkisi tartışılmıştır ve elde edilen sonuçlar literatürdeki diğer çalışmalarla karşılaştırılmıştır.

Sonuç olarak, deneysel numunelerimizin literatürdeki değerlerden daha fazla viskoz ve ısı olarak daha az iletken olduğu bulunmuştur. Bununla birlikte, ölçümlerimizin literatürde yer alan polivinilpirolidon çözeltilerinin sonuçlarıyla daha uyumlu olduğu görülmektedir. Bütün nanoakışkan numunelerin, de-iyonize suya göre yüzde 8.6'ya (25 Watt) kadar iyileştirilmiş bir etkinlik katsayısına sahip olduğu ve sistemin etkinliğinin, tüm ısıtıcı güçlerinde, tanecik konsantrasyonu ve eğim açısının artmasıyla, iyileşme gösterdiği sonucuna varılmıştır.

**Anahtar Kelimeler:** Nanoakışkan, gümüş, yüzey aktif malzemeler, mini döngü, ısı performans, ısı iletkenlik, viskozite, polivinilpirolidon, tek faz, doğal taşınım

## CONTENTS

	<b>Page</b>
M. Sc THESIS EXAMINATION RESULT FORM.....	ii
ACKNOWLEDGEMENTS .....	iii
ABSTRACT .....	iv
ÖZ .....	v
LIST OF FIGURES .....	vii
LIST OF TABLES .....	ix
<b>CHAPTER ONE - INTRODUCTION .....</b>	<b>1</b>
<b>CHAPTER TWO – EXPERIMENTAL APPARATUS AND PROCEDURE ...</b>	<b>10</b>
2.1 Preparation of Nanofluid .....	10
2.2 Thermal Conductivity .....	10
2.3 Viscosity .....	11
2.4 Thermal Performance .....	12
<b>CHAPTER THREE – RESULTS AND DISCUSSIONS.....</b>	<b>15</b>
3.1 Thermal Conductivity of Ag–water Nanofluids .....	15
3.2 Viscosity of Ag–water Nanofluids .....	18
3.3 Thermal Performance of Ag–water Nanofluids in SPNCmL .....	25
<b>CHAPTER FOUR – CONCLUSIONS .....</b>	<b>35</b>
<b>REFERENCES.....</b>	<b>37</b>
<b>APPENDICES .....</b>	<b>48</b>

## LIST OF FIGURES

	<b>Page</b>
Figure 1.1 Number of publications containing the term nanofluid in literature .....	2
Figure 1.2 Illustration of complexity and multivariability of nanofluid systems .2	2
Figure 2.1 Experimental viscosity of water in comparison with ASHRAE Handbook data .....	11
Figure 2.2 Sketch of the experimental setup.....	12
Figure 2.3 Schematic diagram of the experimental set up .....	13
Figure 3.1 Variation of relative thermal conductivity with different Ag nanoparticle concentrations (wt%).....	16
Figure 3.2 Variation of relative thermal conductivity with different Ag nanoparticle concentrations (vol%) compared by Ghanbarpour et al. (2015), Kang et al. (2006), Oliveira et al. (2014), Parammetuwah et al. (2015) and Paul et al. (2012).....	16
Figure 3.3 Variation of relative thermal conductivity with different PVP concentrations (wt%) compared by Dakroury et al. (1990), Xia et al., (2014) and Zhou et al. (2012b) (AT: ambient temperature) .....	18
Figure 3.4 Shear rate and shear stress variation in Ag–water nanofluids with different concentrations (wt%) for 20°C .....	19
Figure 3.5 Shear rate and shear stress variation in Ag–water nanofluids with different concentrations (wt%) for 50°C .....	19
Figure 3.6 Temperature versus viscosity for Ag–water nanofluids at 70 rpm and various concentrations (wt%) .....	20
Figure 3.7 Variation of viscosity with different concentrations (wt%) .....	21
Figure 3.8 Temperature versus relative viscosity for Ag–water nanofluids at 70 rpm and various concentrations (wt%) .....	22
Figure 3.9 Relative viscosity with different Ag nanoparticle concentrations (vol%) compared by Godson et al. (2010), Kang et al. (2006), Karamallah & Sultan (2014) and Oliveria et al. (2012) (AT: ambient temperature, UT: unknown temperature).....	23

Figure 3.10 Variation of relative viscosity with different PVP concentrations (wt%) compared by Fikentscher equation and experimental results of Zhou et al. (2012b) (AT: ambient temperature) .....	24
Figure 3.11 Time dependent variation of $\Delta T_{\text{heater}}$ and $T_{\text{max}}$ at $0^\circ$ inclination angle for DIW .....	26
Figure 3.12 Time dependent variation of $\Delta T_{\text{heater}}$ and $T_{\text{max}}$ at $0^\circ$ inclination angle for 0.25 wt% Ag nanofluid .....	26
Figure 3.13 Time dependent variation of $\Delta T_{\text{heater}}$ and $T_{\text{max}}$ of 0.25 wt% Ag nanofluid for different inclination angle at 20 W .....	27
Figure 3.14 Effectiveness variation as a function of power for DIW and Ag nanofluid with different concentration (wt%).....	28
Figure 3.15 Effectiveness variation for DIW and Ag nanofluid of 0.25 wt% concentration with different inclination angle .....	29
Figure 3.16 Steady state velocity in the SPNCmL versus input power for $0^\circ$ inclination angle .....	31
Figure 3.17 Steady state velocity in the SPNCmL versus input power for 0.25 wt% Ag concentration .....	32
Figure 3.18 Comparison of effectiveness ratio of Ag and $\text{Al}_2\text{O}_3$ nanofluid at $0^\circ$ inclination angle.....	34

## LIST OF TABLES

	<b>Page</b>
Table 2.1 Solution composition (wt%) and density of nanofluid samples .....	10
Table 2.2 Dimensions of loop .....	13
Table 2.3 Thermocouple numbers and positions .....	14
Table 3.1 Summary of information of Doğanay & Turgut (2015) and current experimental investigations on viscosity .....	33



## **CHAPTER ONE**

### **INTRODUCTION**

Conventional heat transfer fluids such as water, oil, ethylene glycol (EG) and soon, could not compensate the needs of advanced thermal engineering technology (Buschmann 2013). Researchers have figured out that the heat transfer is more efficient with usage of the downscaled materials since the pioneering study of Choi (1995). Nanofluids including solid particles in the base fluid had an impact on the field of thermal engineering and brought the heat transfer conundrum into a new light. The heat transfer enhancement capability of nanofluids makes them one of the most suitable materials for thermal engineering studies. Nano scaled metals, metal oxides or carbon based materials mixed into a base fluid to form the nanofluid. Nowadays, nanofluids have the potential for being used in various engineering applications such as solar collectors (Bandarra Filho, Mendoza, Beicker, Menezes, & Wen, 2014; Tyagi, Phelan, & Prasher, 2009), electronics cooling (Hsieh, Leu, & Liu, 2015; Ijam, & Saidur, 2012; Naphon, & Wiriyaart, 2009), nuclear reactor cooling (Barrett, Robinson, Flinders, Sergis, & Hardalupas, 2013), heat exchangers (Godson, Deepak, Enoch, Jefferson, & Raja, 2014; Madhesh, & Kalaiselvam, 2014; Said, Saidur, Sabiha, Hepbasli, & Rahim, 2016), refrigerators (Bi, Guo, Liu, & Wu, 2011; Mahbubul et al., 2014; Saidur, Kazi, Hossain, Rahman, & Mohammed, 2011).

Masuda, Ebata, & Teramae (1993) carried out the first experimental study in respect to thermal conductivity of nanoparticles in base fluid suspensions. They concluded that the  $\text{Al}_2\text{O}_3$ -water nanofluid at concentration of 4.3 percent can increase the thermal conductivity of water by 30 percent. An ongoing research (Choi, Zhang, Yu, Lockwood, & Grulke, 2001; Eastman, Choi, Li, Yu, & Thompson, 2001; Lee, Choi, Li, & Eastman, 1999) corroborated this thermal conductivity enhancement and these results have motivated the researchers to the new experimental and theoretical studies about nanofluids. Just after these motivating results, number of nanofluid related papers has increased expeditiously (Buschmann 2013) as can be seen in Figure 1.1.

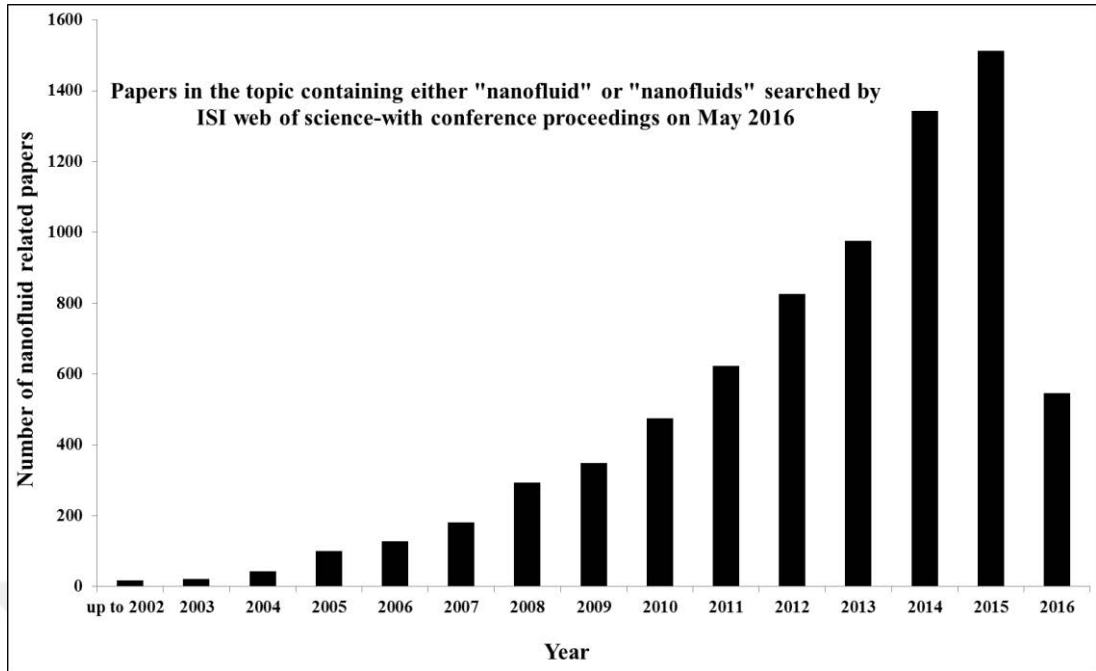


Figure 1.1 Number of publications containing the term nanofluid in literature

In order to advance the understanding of the nano-scale materials effect on systems thermal performance, thermal properties are required for systematical investigations. Thermal conductivity, viscosity, density and heat capacity are important to understand the complexity of nanofluid systems, as shown in Figure 1.2 (Timofeeva, Singh, Yu, & France, 2016).

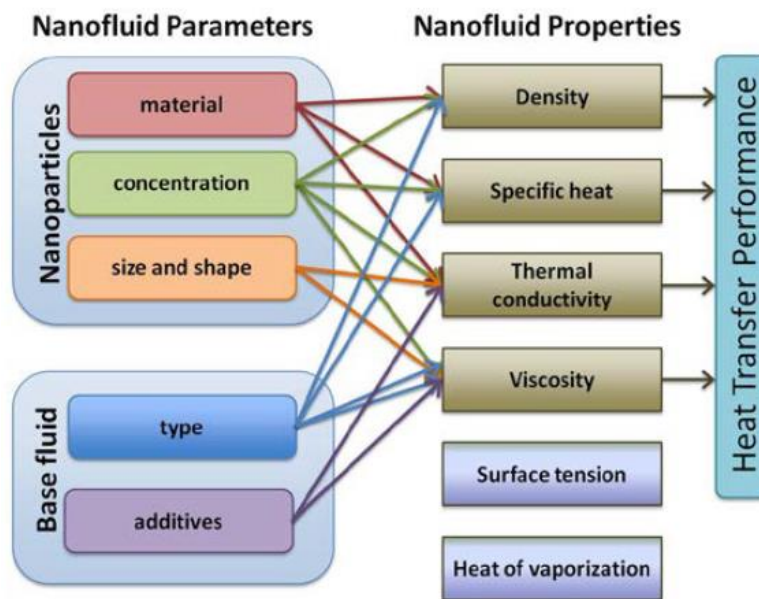


Figure 1.2 Illustration of complexity and multivariability of nanofluid systems (Timofeeva, Singh, Yu, & France, 2016)

Due to their unique electrical, optical and thermal properties, metal nanoparticles such as Ag, Au, Cu and Al, show important recognition in chemistry and physics. Nanofluids including metal nanoparticles are found to have much higher heat transfer potential than nanofluids with metal oxide nanoparticles (Eastman et al., 2001; Murshed, Leong, & Yang, 2005; Sharma, & Jain, 2011). Ag is one of the substantial metals whose potential have been used for nanofluids investigated experimentally for several times. Ag nanoparticles can be chosen due to their high thermal conductivity and stable chemical properties (Zhou, Xia, Chai, Li, & Zhou, 2012a). Capability of being easily synthesized of Ag nanoparticles makes them attractive for nanofluid studies (Haddad, Abid, Oztop, & Mataoui, 2014). Furthermore, Ag is widely accepted as a safe material for human and animals (Salehi, Heyhat, & Rajabpour, 2013).

Many studies are available on the thermal conductivity and viscosity of nanofluids including Ag nanoparticles. Some of these studies include Ag nanofluid without a surfactant (Cho, Baek, Lee, & Park, 2005; Ghanbarpour, Nikkam, Khodabandeh, & Toprak, 2015; Godson, Raja, Lal, & Wongwises, 2010; Karamallah, & Sultan, 2014; Oliveira, Bandarra Filho, & Wen, 2014; Patel et al., 2003, Paul, Sarkar, Pal, Das, & Manna, 2012; Phuoc, Soong, & Chyu, 2007), while some of them used a surfactant which can overcome the stabilization problem by preventing agglomeration. (Iyahraja, & Rajadurai, 2015; Kang, Kim, & Oh, 2006; Karthikeyan, Ramachandran, Pillai, & Solomon, 2014; Li, Hong, Fang, Guo, & Lin, 2010; Parametthanuwat, Bhuwakietchumjohn, Rittidech, & Ding, 2015; Salehi et al., 2013; Singh & Raykar 2008; Warriar, & Teja, 2011; Zhou et al., 2012a; Zhou, Xia, & Chai, 2015).

A silver nanofluid was synthesized for the first time by citrate reduction route in the study of Patel et al. (2003). They concluded that the thermal conductivity of Ag–citrate nanofluids with 60–80 nm particle size enhances from about 3.2% to 16.5% at 30–60°C temperature range. Cho et al. (2005) utilized the chemical reduction method for preparation of Ag–EG nanofluids which enhances the thermal conductivity up to 18% for the concentration of 5000 ppm. Paul et al. (2012) prepared Ag–water nanofluid with 55 nm particle size by wet chemical bottom up

approach. They reported that maximum thermal conductivity enhancement of Ag nanofluid is at 0.1 vol%. Phuoc et al. (2007) produced Ag nanofluid with one step method as laser ablation of metal targets in water solutions without use of any dispersants or surfactant. Their results indicated that the viscosity increases 3.7% and the thermal conductivity increases about 3–5% for 0.01 vol% concentration. Godson et al. (2010) prepared their Ag–water nanofluid samples at volume concentrations from 0.3% to 0.9% without using any surfactant. They reported that the thermal conductivity of Ag nanofluids increases as the temperature increases from 50 to 90°C. On the contrary, the viscosity of nanofluids decreases with the increase in temperature. Moreover, they investigated the effect of Brownian motion on the thermophysical properties of nanofluid. They demonstrated that the Brownian velocity increases by 40–60% with every 0.3% concentration increase. Oliveira et al. (2014) performed an experimental study with Ag–water nanofluid by altering the volume concentration between 0.1–0.3% with two different particle sizes (10 and 80 nm). Their results showed that the relative viscosity ( $\mu_{nf}/\mu_{bf}$ ) and the relative thermal conductivity ( $k_{nf}/k_{bf}$ ) of Ag–water nanofluid does not reveal a systematic behavior response to the particle size. They also concluded that the thermal conductivity increases with the volume concentration; however the viscosity of nanofluid shows an inconsistent trend with the increase of concentration. Karamallah et al. (2014) reported that the Ag nanofluid behavior is close to Newtonian fluids through the function between shear rate and viscosity. Moreover, the experimental viscosity data is much larger than the theoretical model values. They also mentioned that the enhancement can be attributed to the specific surface areas of the nanoparticles. When the particle size of Ag nanoparticles is less than 20 nm, the viscosity of nanofluid will increase rapidly with decreasing particle sizes.

Due to high surface energy of the nanoparticles, the nanofluids have tendency to aggregate which causes instabilities and quick settling down of the particles. Addition of surfactants into base fluids is generally used to minimize aggregation and enhance dispersion of nanoparticles. On the other hand, surfactants influence the thermal properties of liquids, such as, thermal conductivity and viscosity (Hwang et al., 2008; Iyahraja, & Rajadurai, 2015; Timofeeva, Routbort, & Singh, 2009; Zhou,

Xia, Li, Chai, & Zhou, 2012b). Chen & Xie (2010) concluded that cationic gemini surfactant is a negative factor in improving the thermal conductivity at higher concentrations. Tavman & Turgut (2010) found that the thermal conductivity of sodium dodecyl benzene sulfonate (SDBS)–water suspension decreases with the increasing SDBS ratio which expresses the surfactant effect on thermal conductivity.

Polyvinylpyrrolidone (PVP) prevents nanoparticle aggregation and control the average particle size and shape as providing a steric barrier on particle surface (Goel, & Rani, 2012; Zhang, Zhao, & Hu, 1996). PVP is widely used in the synthesis of Ag nanofluids. Moreover, PVP is distinguished from the other surfactants thanks to its good solubility in polar solvents and thermal stability (Abdelrazek, Ragab, & Abdelaziz, 2013; Xia, Jiang, Liu, & Zhai, 2014). Dakroury, Osman & El-Sharkawy (1990) obtained that the concentration of PVP in aqueous solutions affects the thermal properties of the solution. As the concentration of the surfactant rises, the viscosity of fluid increases which leads to decrease in the thermal conductivity of the fluid ( $\mu.k=\text{constant}$ ). Sweil & Talbot (2002) measured the viscosity of aqueous PVP solutions with different concentrations from 2 to 3 wt% considering  $K$ -values which is a function of the average molecular weight. They resulted that the viscosity of this suspension increases for each weight percent of PVP. Yu, Xie, Chen & Li (2010) found that the surfactant addition might be led to negative effect on thermal conductivity. When they added the PVP with 5% weight concentration, the thermal conductivity of PVP/EG suspension decreases about 2% compared to EG. Zhou et al. (2012b) experimentally investigated the viscosity and thermal conductivity of different common surfactant as SDBS, sodium dodecyl sulfate (SDS), cetyltrimethylammonium bromide (CTAB) and PVP solutions. They concluded that all of these surfactants reach a stable thermal conductivity ratio (the ratio of the thermal conductivity of the surfactant solution to that of the water) after a certain concentration. PVP seems to be more special than the others due to its thermal conductivity ratio decreases rapidly reaching the lowest value at 0.1 wt%, and then increases gradually with increasing concentration. Moreover, the viscosity of PVP solution is significantly higher than the solution including the other surfactant at 20°C and decreases quickly with increase in temperature. They reported

that the special thermal properties of PVP solution is related to the long alkyl chain molecules which winds with each other.

Kang et al. (2006) worked on Ag–water nanofluid with 8–15 nm particle size and volume concentrations of 1%, 2% and 3%. Although the surfactant was added to disperse particles into fluid, the type of surfactant was not mentioned. They reported that the viscosity of nanofluids increases 30% at 2 vol% and the thermal conductivity increases 11% at 4 vol% compared to those of the base fluid. Singh & Raykar (2008) prepared silver nitrate ( $\text{AgNO}_3$ )–ethanol nanofluid using PVP as surfactant with weight ratio of 1:10, 1:5 ( $\text{AgNO}_3$  to PVP). They reported that the nonlinear behavior of relative thermal conductivity of nanofluids can be explained based on Brownian motion of nanoparticles. As temperature increases, diffusion rate of nanoparticles increases due to the loss of polymer binding (Das, Putra, Thiesen, & Roetzel, 2003). Moreover, they also concluded that the thermal conductivity enhancements greater than 1.55 for sample with PVP weight ratio 1:5 at temperature 323 K.

Li et al. (2010) prepared Ag–oil nanofluids with using the oleic acid to coat the surface of Ag nanoparticles. They concluded that the thermal conductivity of nanofluid is higher than the base fluid and increases nonlinearly with increasing weight concentration of the nanofluid. Moreover, the thermal conductivity enhancement of the nanofluid at room temperature is much less than those at higher temperatures. They deduced that the results can be related to the capping of the surfaces of the nanoparticles with oleic acid. As heat transfer in solid and base liquid suspensions occurs at the interface of the solid particle and the fluid interface, an increase in the size of interfacial area can lead to more efficient heat transfer properties (Karthikeyan et al., 2008). Warriar et al. (2011) examined the particle size effect on the thermal conductivity of Ag–EG nanofluid with three different sizes (20, 30–50 and 80 nm) at 1 and 2 vol% concentration of 0.3 wt% PVP as surfactant was used to keep the particles as well-dispersed in the base fluid. They concluded that the results appear to support the thermal conductivity of Ag–EG nanofluid decreases with decreasing particle size. Salehi et al. (2013) reported that the amount of PVP in Ag–water nanofluids can have a significant effect on thermal conductivity. Their

results indicated that the thermal conductivity decreases with an increase in the amount of PVP above 500 ppm particle concentrations. Xia et al. (2014) investigated the effects of PVP on stability of  $\text{Al}_2\text{O}_3$ –water nanofluids and reported that the addition of PVP has negative influence on thermal conductivity of base fluid and significantly improves the stability of nanofluid. Zhou et al. (2012a) studied on Ag nanofluids with different volume concentrations suspended into a 12 g/L PVP-water solution through the micro-pin fin heat sink. They reported that the heat transfer capability has improved significantly with the addition of Ag nanoparticles. But, the thermal resistance of Ag nanofluids under different conditions of pumping power is higher than de-ionized water at low particle volume concentration. They ascribed these results to the addition of surfactant PVP, which induces two disadvantageous roles: decreasing thermal conductivity and increasing viscosity of nanofluids. After a three years period, Zhou et al. (2015) made an experimental effort on measuring the same nanofluid in the pin–fin heat sinks. They obtained similar viscosity values with the previous one. The viscosity of base fluid is higher than the water by 30% and when a small amount of Ag nanoparticles is added, there is no apparent change of viscosity. Because of the weakened effect of PVP in nanofluids, only when the Ag nanoparticle reaches 0.12 wt%, the heat transfer performance is better than water with an enhancement of 6.61%. Moreover, they reported that if the concentration of PVP is too high, long PVP chain will wind each other and Ag nanoparticles will aggregate easily. Therefore, PVP concentration should be controlled at a proper value. To obtain more accurate results about effect of surfactants, Iyahraja & Rajadurai (2015) added SDS and PVP as surfactants. The mass concentration ratio of surfactant to Ag nanoparticles was varied from 1:10 to 1:2. They deduced that the surfactants have a significant role on the thermal conductivity enhancement of nanofluids. As the PVP concentration increases, the thermal conductivity enhancement of Ag–water nanofluid decreases. With the addition of 0.5 wt% PVP, the enhancement of thermal conductivity of nanofluid sample reduced by 9.7% compared to the sample without surfactant (Iyahraja, & Rajadurai, 2015).

Natural circulation loops (NCLs) are heat transport systems, in which the fluid motion is generated by density difference occurring due to phase change or

temperature gradients without any external power source (pump, fan, suction device etc.). NCLs could be considered as two-phase NCL (TPNCL) or single-phase NCL (SPNCL) whether density gradient is caused by a phase change or temperature gradient, respectively. Due to its disadvantages such as complex design, instabilities and requirement of precision control, two-phase NCLs have restricted application range. On the contrary, the SPNCLs have widespread application thanks to its enhanced safety, simplicity and reliability (Basu, Bhattacharyya, & Das, 2012). Two basic approaches became prominent for improving cooling technology: maximize the cooling performance and decrease the characteristic dimensions (Jang, & Choi, 2006). In order to keep a SPNCL in the stable zone, Basu, Bhattacharyya & Das (2013) decreased the horizontal arm length, vertical arm length and pipe inner diameter. They reported that the loop with smaller diameter is found to be more stable due to enhanced friction.

Until now, several studies (Doğanay, & Turgut, 2015; Misale, Devia, & Garibaldi, 2012; Nayak, Gartia, & Vijayan, 2008; Nayak, Gartia, & Vijayan, 2009; Turgut, & Doğanay, 2014;) have examined the thermal performance of nanofluid on SPNCLs. Nayak et al. (2008) investigated experimentally behavior of a large scaled SPNCL with water and  $\text{Al}_2\text{O}_3$ -water nanofluid with different concentrations (0.3–2 wt% and 40–80 nm nanoparticle size). Their results showed that natural circulation flow rate is enhanced with using nanofluid. Moreover, they reported that the system efficiency increases with increasing nanoparticle concentration, however suppression of instabilities decreasing. A year later, Nayak et al. (2009) conducted their experiments with three different metallic oxide nanofluids (0.5% by wt.) as  $\text{Al}_2\text{O}_3$ , CuO and  $\text{TiO}_2$  having particle size of 60, 50 and 25 nm, respectively. They concluded that the  $\text{Al}_2\text{O}_3$  and  $\text{TiO}_2$  nanofluids seem to be more promising over the entire power range. Findings of both study indicated that the SPNCLs are potential systems for the thermal management of electronic devices. Misale et al. (2012) tested the thermo-hydraulic performance of a single-phase natural circulation mini loop (SPNCmL) whose dimensions are 180x264 mm in lengths and 4 mm in internal diameter. The experiments were first performed with using DIW and then  $\text{Al}_2\text{O}_3$ -water nanofluids with volume concentrations of 0.5% and 3%. Moreover, they investigated the

varying parameters such as input power (10 to 50 W), inclination angle of loop ( $0^\circ$  to  $75^\circ$ ) and heat sink temperature (10 and  $20^\circ\text{C}$ ). They only obtained a slight thermal performance enhancement with nanofluids at  $75^\circ$  inclination angle. Turgut & Doğanay (2014) made an experimental effort with a SPNCmL for  $20^\circ\text{C}$  heat sink temperature and  $0^\circ$  inclined angle by altering applied power in the range of 10 to 50 W. They concluded that the thermal performance of  $\text{Al}_2\text{O}_3$ –water nanofluids shows an enhancement with increasing input power and particle concentration. They also pointed out that all the nanofluid samples have higher thermal performance than the DIW. After one year, Doğanay & Turgut (2015) again with the same setup made experiments for different inclination angles. Contradictory to the results of Misale et al. (2012), they showed that using nanofluids enhances the thermal performance of SPNCmL for the inclination angles from  $0$  to  $75^\circ$ .

In this study, the thermal performance of Ag–water nanofluid in a SPNCmL was investigated experimentally. Obtained results were compared with the results of Doğanay & Turgut (2015) which includes  $\text{Al}_2\text{O}_3$ –water nanofluid in the same system. Moreover, the thermal conductivity and viscosity of Ag–water nanofluid were measured by  $3\omega$  method and Brookfield Viscometer, respectively. Additionally, the influence of PVP on thermal conductivity, viscosity and thermal performance of Ag-water nanofluid has been discussed.

## CHAPTER TWO

### EXPERIMENTAL APPARATUS AND PROCEDURE

#### 2.1 Preparation of Nanofluid

The Ag-water nanofluid with 5 wt% concentration of 15 nm spherical Ag nanoparticles, which contains 1.25 wt% PVP was procured from US Research Nanomaterials, Inc. (Houston, USA). Then, these 5 wt% nanofluids were diluted to 4 different weight concentrations, namely 0.25%, 0.5%, 0.75% and 1%. To obtain a uniform dispersion, each sample was stirred for 10 minutes duration after dilution process. Concentration and type of surfactant was found to be sufficient to keep the suspension stable even after 6 months.

Concentration of Ag, PVP and the density of nanofluids are shown in Table 2.1. The density of nanofluid ( $\rho_{nf}$ ) and base fluid ( $\rho_{bf}$ ) was measured by taking constant  $10\pm 0.1$  ml and then weighed on a high precision (Precisa XB 220A) microbalance ( $\pm 0.001$  g).

Table 2.1 Solution composition (wt%) and density of nanofluid samples

Solution composition wt%		Density (kgm <sup>-3</sup> ) (23°C)
Ag	PVP	
water	0	964.67
0.25	0.0675	973.89
0.5	0.125	986.57
0.75	0.1875	997.57
1	0.25	1009.05

#### 2.2 Thermal Conductivity

Thermal conductivity of nanofluids was measured by  $3\omega$  lock-in detection at ambient temperature (23°C).  $3\omega$  method was first presented in 1990 by Cahill and has gained importance for the characterization of thermal properties in parallel with improvement in nanotechnology. The popularity of this method has increased with

the interest in thermal conductivity of thin films. The method was validated with pure fluids, such as water, ethylene glycol methanol, and ethanol and yielding accurate thermal conductivity ratios within  $\pm 2\%$ . The details of experimental setup of the technique have been explained with details previously (Tavman, & Turgut, 2010; Turgut et al., 2008). Thermal conductivity of water was measured to be 0.6 W/mK. Relative thermal conductivity parameter is defined as thermal conductivity of nanofluid/base fluid ratio. In the case of relative measurements, the resolution is 0.1% in thermal conductivity.

### 2.3 Viscosity

The viscosity of samples was measured by using a Brookfield Viscometer which had an UL (ultralow) adapter and UL spindle in order to measure viscosity values lower than 15 cP. Applied torque was kept in the range of 10–100% in order to carry out reliable viscosity measurements (Turgut, Sağlanmak, & Doğanay, 2016). After each measurement, spindle was cleaned off by using alcohol and pure water, respectively. The temperature variation (from 20 to 50°C) of samples was supplied by temperature bath (Polyscience M9712, USA).

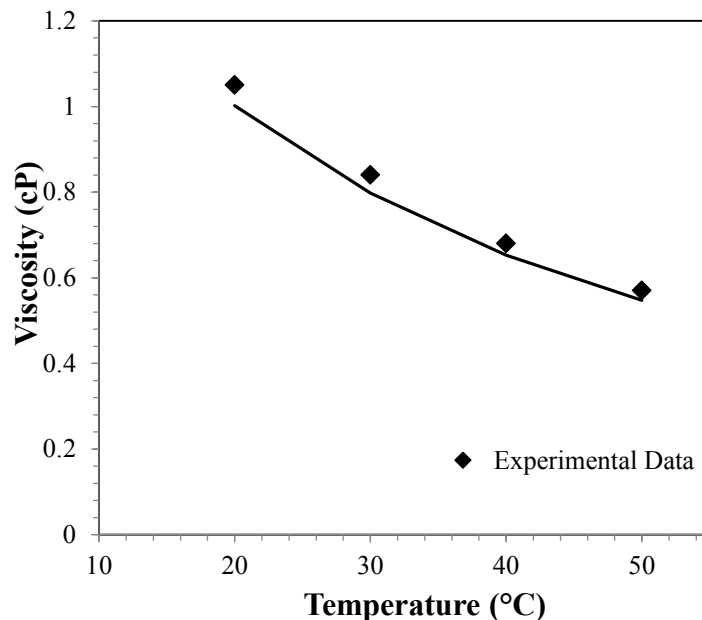


Figure 2.1 Experimental viscosity of water in comparison with ASHRAE Handbook (1985) data

The accuracy of viscosity measurement was verified by comparing the measured water as base fluid value with the ASHRAE handbook (American Society of Heating, Refrigerating and Air-Conditioning Engineers Handbook, 1985). The maximum deviation was found as 4% (Figure 2.1).

## 2.4 Thermal Performance

The design of experimental setup was mentioned in Turgut & Doganay 2014. The mini loop has a rectangular shape (304 mm x 220 mm) which consist of copper pipes with 4.75 mm inner diameter connected with four glass bends (Figure 2.2).

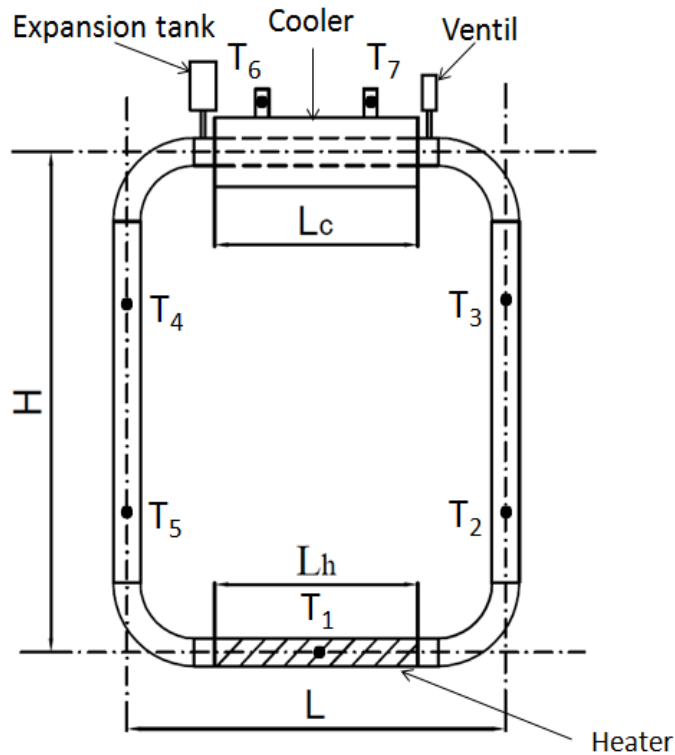


Figure 2.2 Sketch of the experimental setup

An expansion tank placed on the top side to prevent the system from the excessive pressures. To supply or extract working fluid, a ventil was added. The expansion tank and ventil are also made by copper pipes with inner diameters of 19 mm and 10 mm, respectively (Table 2.2).

Table 2.2 Dimensions of mini loop

Parameter	Dimension (mm)
$D_{tube}$	4.75
$D_{expansion\ tank}$	19
$D_{ventil}$	10
$H$	304
$L$	220
$L_c$	110
$L_h$	140

A heater consists of an electrical resistance with  $1.77 \Omega/m$  was positioned at the bottom of the system. The coaxial heat exchange system positioned at the top side of the system as a cooler fed by a bath circulator (Polyscience M9712) at  $20^\circ\text{C}$  temperature with  $0.01^\circ\text{C}$  stability.

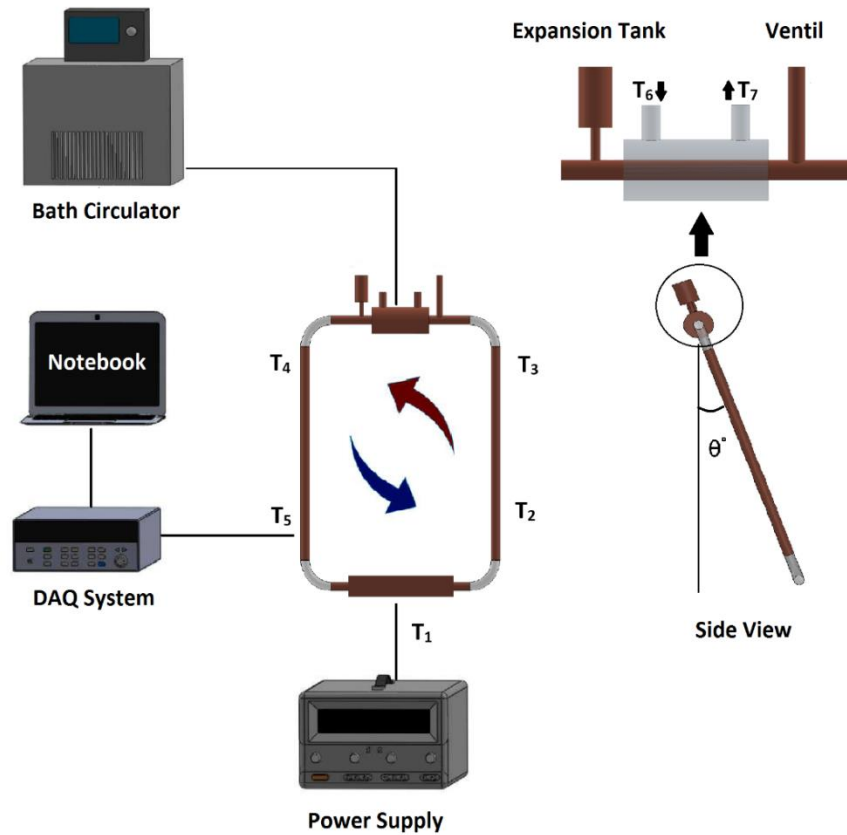


Figure 2.3 Schematic diagram of the experimental set up

Figure 2.3 shows a diagram of this experimental setup. The loop is mounted on a table by using four pipe clamps. Two special screws adjust the table to provide the rotation around the  $x$ -axis for the desired inclination angle.

The power supply voltage and the bath temperature were kept constant throughout each experiment. The fluid temperature in mini-loop was recorded by regular interval using thermocouples of type-K (Omega Engineering, USA) connected to a data logger (HP34970A, 0.01°C resolution). Thermocouple numbers and positions are indicated in Table 2.3. The accuracy of the thermocouples was obtained as  $\pm 0.05$  °C by water bath calibration of thermocouples.

Table 2.3 Thermocouple numbers and positions

<b>Thermocouple</b>	<b>Position</b>
$T_1$	Heater
$T_2$	Outlet side of heater
$T_3$	Inlet side of cooler
$T_4$	Outlet side of cooler
$T_5$	Inlet side of heater
$T_6$	Inlet of cooler
$T_7$	Outlet of cooler

Power supply and water bath were activated simultaneously after 100 s from the data acquisition started. After each termination, it is waited for the system to return to the steady-state conditions. The experiments were conducted by varying two parameters such as heater power between 10 and 50W and inclination angle of the system at 0°, 30° and 60°. The mini loop was cleaned regularly with pure water because the nanoparticles could settle on the inner surface of pipes.

To ascertain the repeatability of the experimental results, all measurements of thermal conductivity, viscosity and thermal performance experiments were repeated at certain intervals (once every two days) at least thrice. All of the measurements were performed first with de-ionized water (DIW) and then with nanofluid samples.

## CHAPTER THREE

### RESULTS AND DISCUSSIONS

#### 3.1 Thermal Conductivity of Ag–water Nanofluids

The relative thermal conductivity ( $k_{nf}/k_{bf}$ ) of Ag–water nanofluids with concentrations of 0.25, 0.5, 0.75 and 1 wt% were measured at ambient temperature (23°C). It is clearly seen from Figure 3.1, the thermal conductivity of our sample decreases with increasing the concentration of nanoparticles. It is found that the relative thermal conductivity decrement of nanofluid increases from 3 to 11.5% with increasing concentration from 0.25 to 1 wt%.

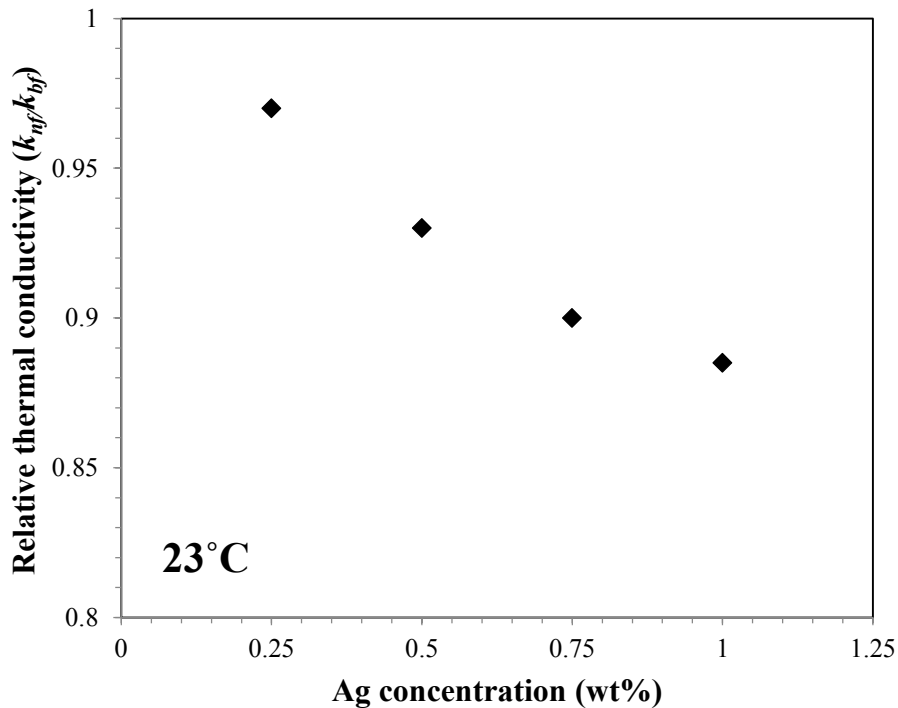


Figure 3.1 Variation of relative thermal conductivity with different concentrations (wt%)

The classical models such as Maxwell (1981), Bruggeman (1935) and Hamilton & Crosser (1962) fail to predict the effective thermal conductivity of nanofluids, as reviewed by Murshed & de Castro (2014) and Kleinstreuer & Feng (2011), because such models include effect of particle concentration generally (superficially??), and they have been basically developed for composites and micro or milli-sized

inclusions (Vanaki, Ganesan, & Mohammed, 2016). Due to the fact that the effect of surfactant was not included enough in these models, a complete model on thermal conductivity of nanofluids has not been succeeded yet.

Our results show a contradiction with the thermal conductivity data to the data reported in the literature. Figure 3.2 illustrates the comparison between our measurement results and experimental thermal conductivity values of the available studies (Ghanbarpour et al., 2015; Kang et al., 2006; Oliveira et al., 2014; Parammettuwah et al., 2015; Paul et al., 2012) which investigated Ag nanofluid (without using PVP) as a function of volume concentration (vol%).

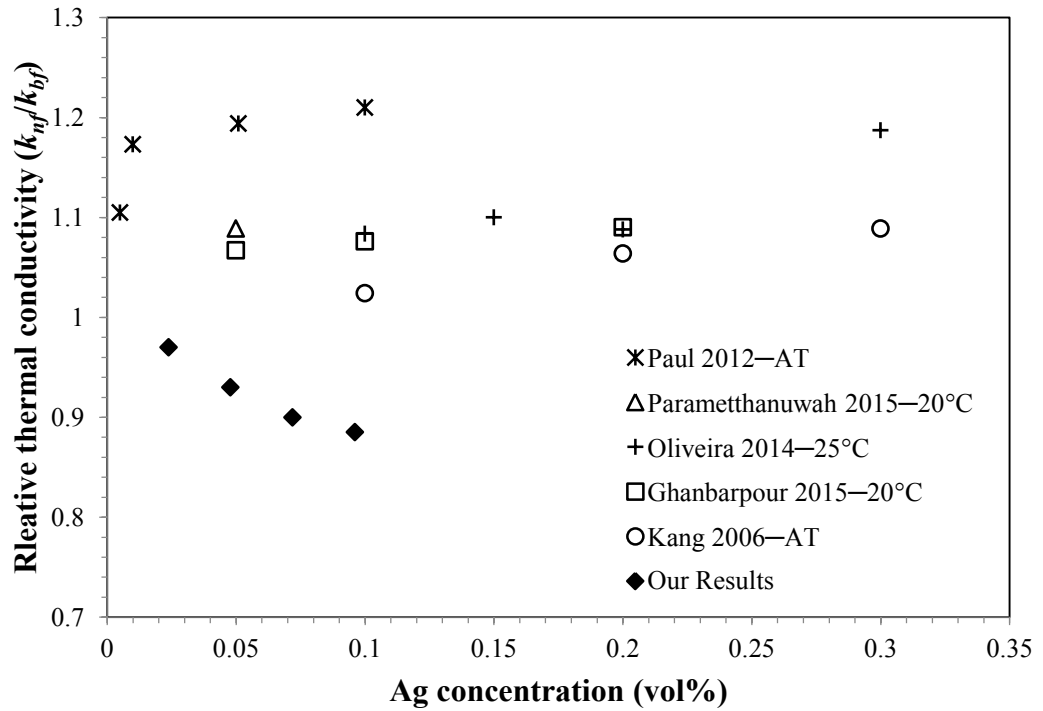


Figure 3.2 Variation of relative thermal conductivity with different Ag nanoparticle concentrations (vol%) compared by Ghanbarpour et al. (2015), Kang et al. (2006), Oliveira et al. (2014), Parammettuwah et al. (2015) and Paul et al. (2012)

The volume concentrations ( $\phi_{vol}$ ) were calculated using weight concentrations ( $\phi_{wt}$ ) and the densities of nanoparticle ( $\rho_{np}$ ) and base fluid ( $\rho_{bf}$ ) (Eq. 3.1).

$$\phi_{vol} = \frac{1}{1 + \left( \frac{1}{\phi_{wt}} - 1 \right) \left( \frac{\rho_{bf}}{\rho_{np}} \right)} \quad (3.1)$$

As seen in Figure 3.2, it is widely accepted that the thermal conductivity of nanofluid is greater than that of the base fluid in which the nanoparticles dispersed. However, it is known that the surfactants tend to weaken the thermal conductivity of its base fluid. Iyahraja & Rajadurai (2015) investigated the effect of the concentration of PVP on the thermal conductivity enhancement of nanofluid. They reported that the addition of surfactant prevents the contact between the successive two particles as the repulsive force dominates the attractive force of the particles. They also concluded that the thermal conductivity enhancement of the nanofluid becomes lower because of the increase in the concentration of the PVP. Dakroury et al. (1990) associated the decrease in thermal conductivity with the decrease in the mean free path of PVP molecules due to the increasing PVP concentration. Therefore, a low thermal conductivity of Ag–water nanofluid can be related with the use of PVP. Xia et al. (2014) concluded that PVP has negative influence on thermal conductivity of base fluid. On the other hand, Zhou et al. (2012b) mentioned that the thermal conductivity of PVP gradually approaches the value of de-ionized water with increasing temperature. The reason of this behavior can be attributed to the loss of PVP polymer binding with increasing temperature (Singh, & Raykar, 2008). Since our existing experimental setup is not sufficient for thermal conductivity measurements at high temperatures, the effect of temperature on the PVP could not be obtained experimentally. Figure 3.3 shows a comparison between the results of our study and those of the previous reports (Dakroury et al., 1990; Xia et al., 2014; Zhou et al., 2012b) which investigated the aqueous solutions of PVP. The qualitative similarity of curves may be related with that the Ag nanoparticles cannot reveal their potential due to the fact that PVP has a strong barrier effect on surface of the particles at ambient temperature (23°C).

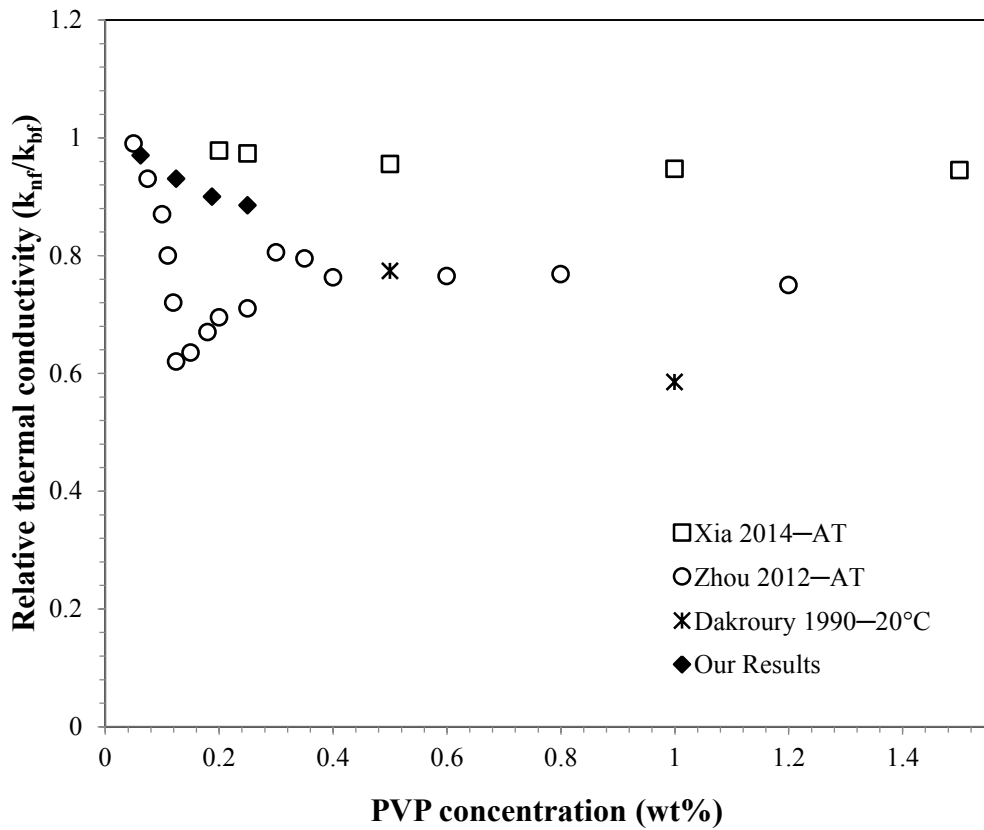


Figure 3.3 Variation of relative thermal conductivity with different PVP concentrations (wt%) compared by Dakroury et al. (1990), Xia et al. (2014) and Zhou et al. (2012b) (AT: ambient temperature)

### 3.2 Viscosity of Ag–water Nanofluids

The viscosity of nanofluids was measured in the temperature range of 20°C and 50°C. Figure 3.4 and Figure 3.5 show the shear stress versus shear rate values of Ag–water nanofluid with various concentrations at lowest and highest temperature, respectively. Liquids with low viscosity cannot be measured at high shear rate because of the low torque (Figure 3.5). For both temperatures of 20°C and 50°C, there is a linear relationship ( $0.998 < R^2 < 1$ ) between shear stress and shear rate, which shows Newtonian fluid behavior for all samples. Until now, several studies have experimented the viscosity of water based Ag nanoparticle with using PVP (Zhou et al., 2012b) and without using PVP (Godson et al., 2010; Karamallah, & Sultan, 2014; Oliveria et al., 2012). As a result, all these studies showed that the viscosity curves of nanofluids are close to the typical Newtonian behavior. Moreover, the PVP–water

suspension shows the same linear behavior (Swei, & Talbot, 2002; Zhou et al., 2012b).

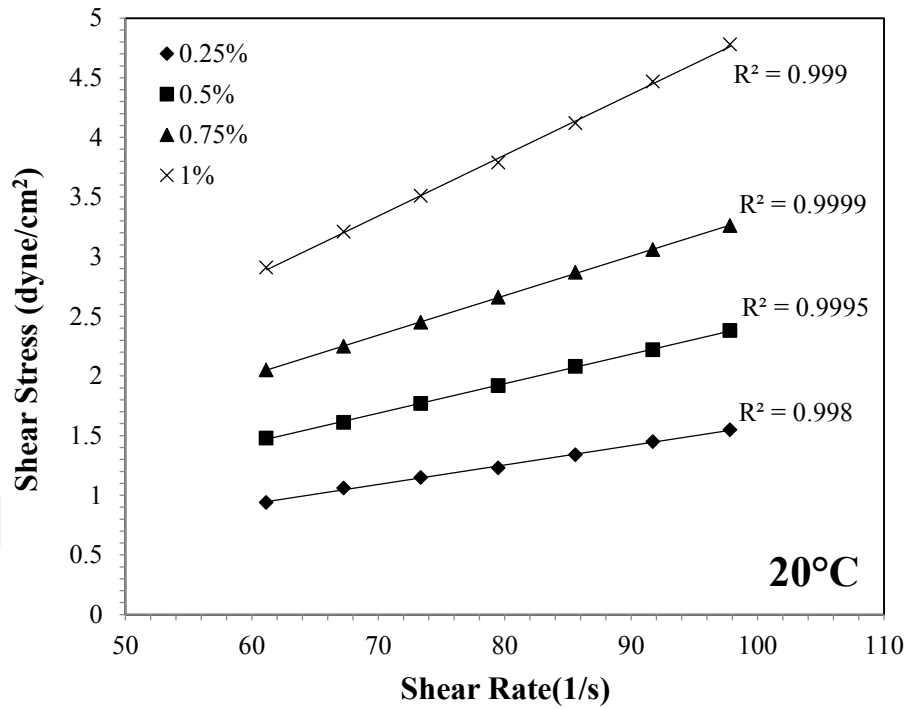


Figure 3.4 Shear rate and shear stress variation in Ag–water nanofluids with different concentrations (wt%) for 20°C

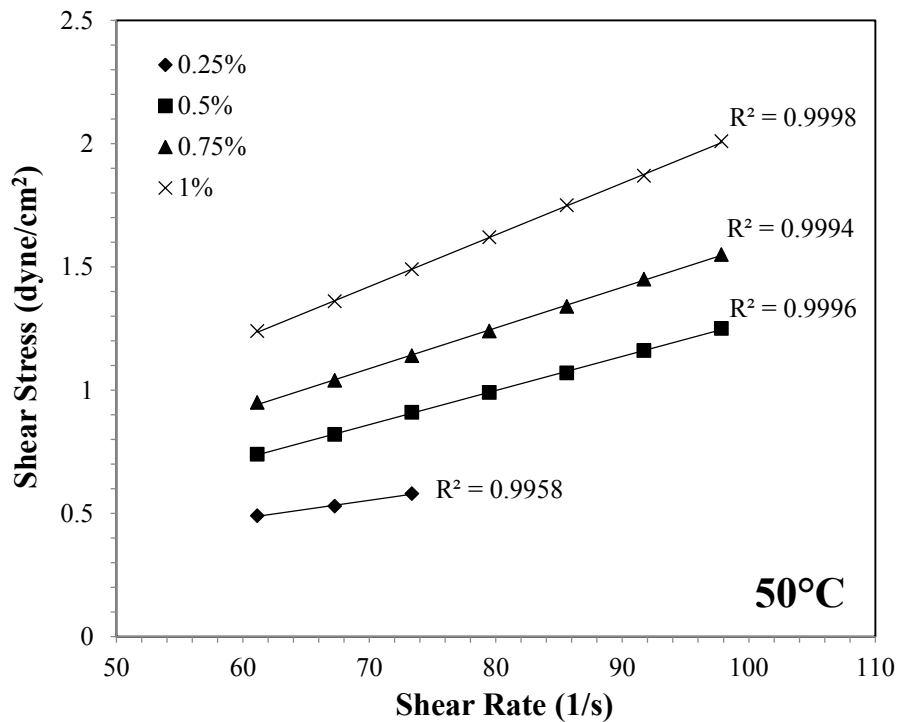


Figure 3.5 Shear rate and shear stress variation in Ag–water nanofluids with different concentrations (wt%) for 50°C

The influence of temperature and nanoparticle concentration on the viscosity of nanofluids at 70 rpm shear rate is shown in Figure 3.6. It is shown that the viscosity of Ag–water nanofluid shows a decrement with increasing temperature. As mentioned by Mahbubul et al. (2014), with the temperature increases, viscosity of liquids decreases due to the reduction of attractive forces between molecules.

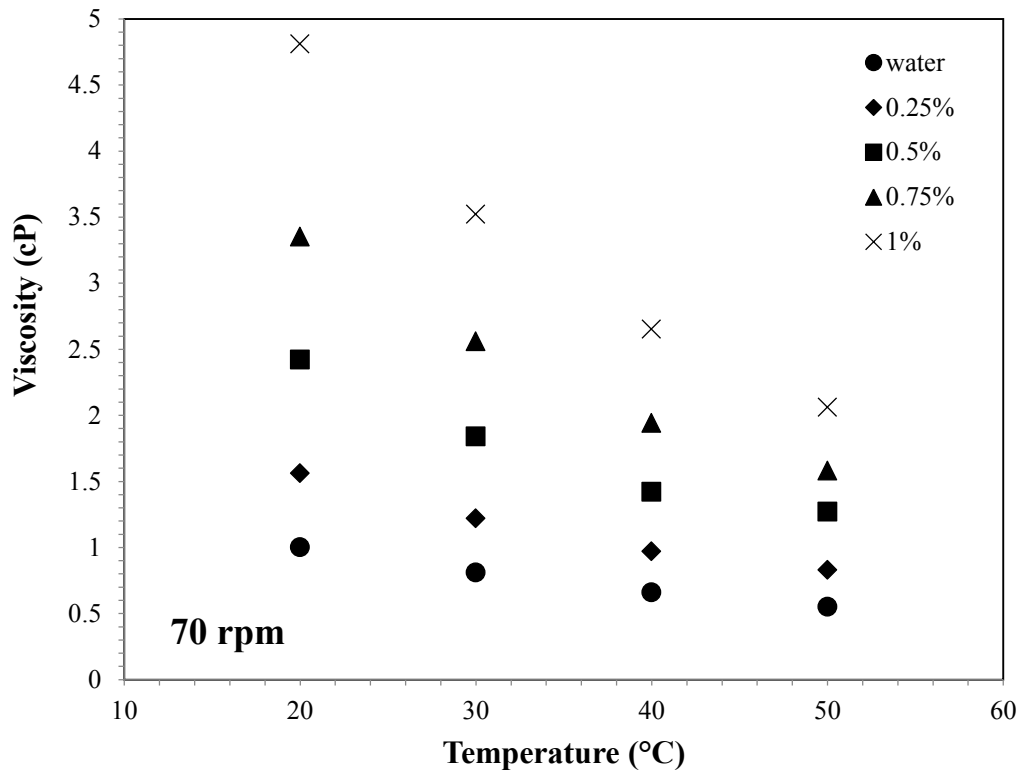


Figure 3.6 Temperature versus viscosity for Ag–water nanofluids at 70 rpm and various concentrations (wt%)

Figure 3.7 represents the viscosity of the Ag–water nanofluids with different concentrations. It is indicated that the viscosity of nanofluids increases with increasing weight concentration of nanoparticle. The enhancement in viscosity of 0.25, 0.5, 0.75 and 1 wt% Ag–water nanofluids are found to be 46%, 123%, 210% and 343% respectively, at ambient temperature (23°C).

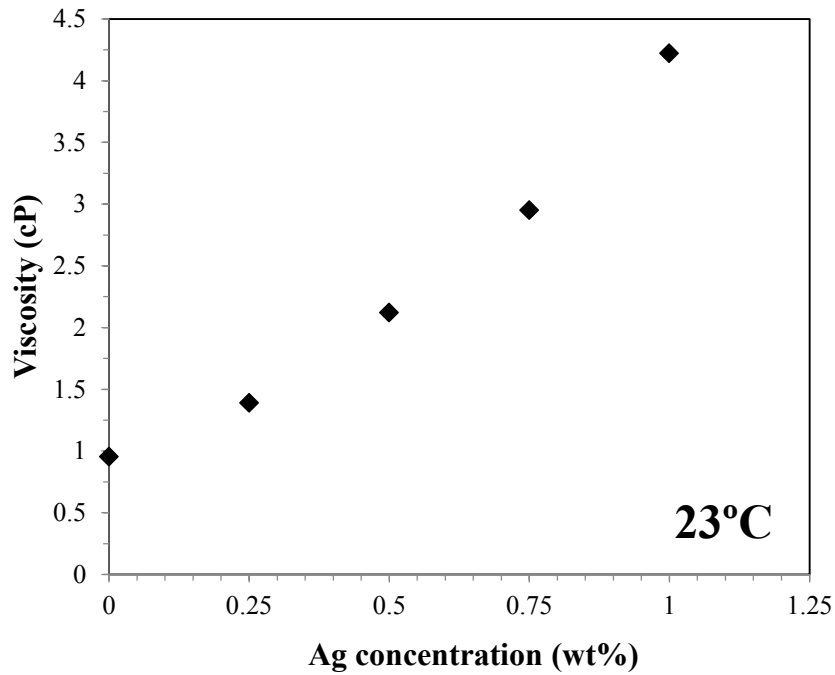


Figure 3.7 Variation of viscosity with different concentrations (wt%)

Many studies have reported that the classical models fail to explain the viscosity of nanofluid because of the missing parameters (Mahbubul, Saidur, & Amalina, 2012; Murshed, Leong, & Yang, 2008; Sundar, Sharma, Naik, & Singh, 2013). Due to the fact that there is no unique model which includes the effects of particle size, concentration, aggregation, surfactant and temperature simultaneously; our results were not compared with the existing models.

For a better discussion of the temperature effect on viscosity of nanofluids, viscosity values were normalized with de-ionized water (Figure 3.8). The relative viscosity ( $\mu_{nf}/\mu_{bf}$ ) of Ag–water nanofluid with 1 wt% concentration is found to be 4.81, 4.35, 4.02, and 3.75 for 20, 30, 40 and 50°C, respectively. As for the nanofluid with 0.25 wt% concentration, relative viscosity is found to be 1.56, 1.51, 1.47 and 1.51 for 20, 30, 40 and 50°C, respectively. It is concluded that the relative viscosity of higher concentration samples shows a dramatic decrease whereas it is almost stable for the lower concentrations. The relative viscosity ratio of 1 and 0.25 wt% samples decreases from 4.81 to 3.75 and from 1.56 to 1.51, respectively. This provides the information that for the lower concentrations of Ag and PVP, samples behave similar to water according to temperature. However, for the higher

concentrations, temperature effect is more significant on the decrease of the relative viscosity.

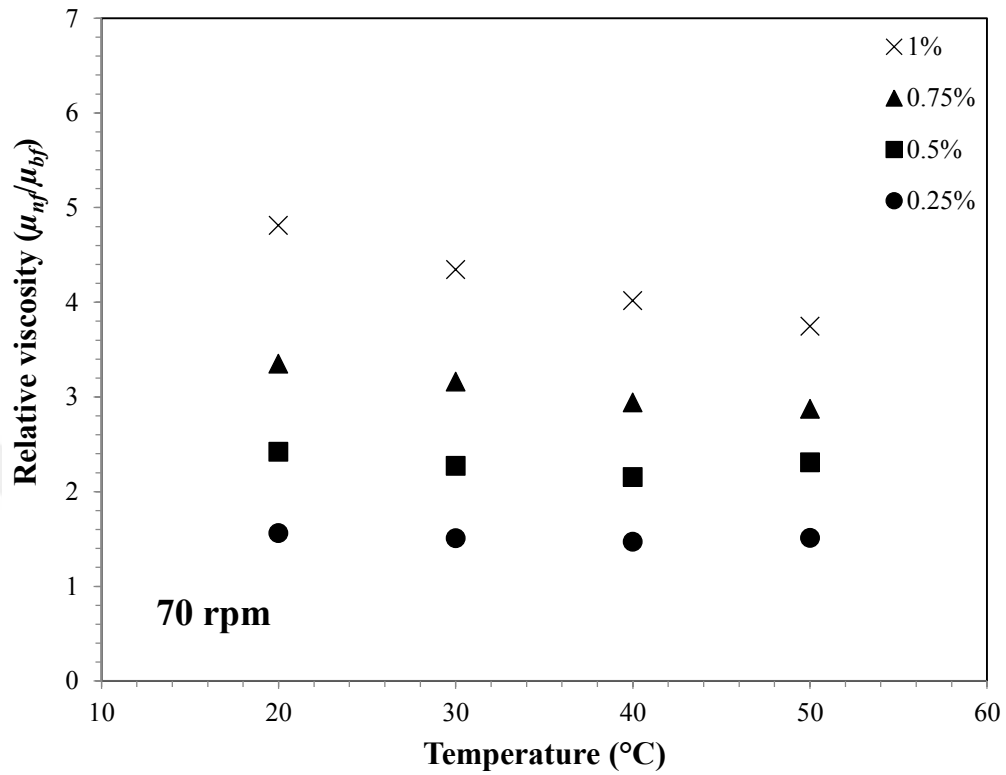


Figure 3.8 Temperature versus relative viscosity for Ag–water nanofluids at 70 rpm and various concentrations (wt%)

As seen in Figure 3.9, the relative viscosity ( $\mu_{nf}/\mu_{bf}$ ) of nanofluids is found to be increased anomalously with increasing volume concentration in comparison with references (Godson et al., 2010; Kang et al., 2006; Karamallah, & Sultan, 2014; Oliveria et al., 2012) including Ag–water nanofluid without using PVP. There is an agreement in the literature that the relative viscosity of Ag-water nanofluids, as a function of concentration, has generally lower values than our experimental results.

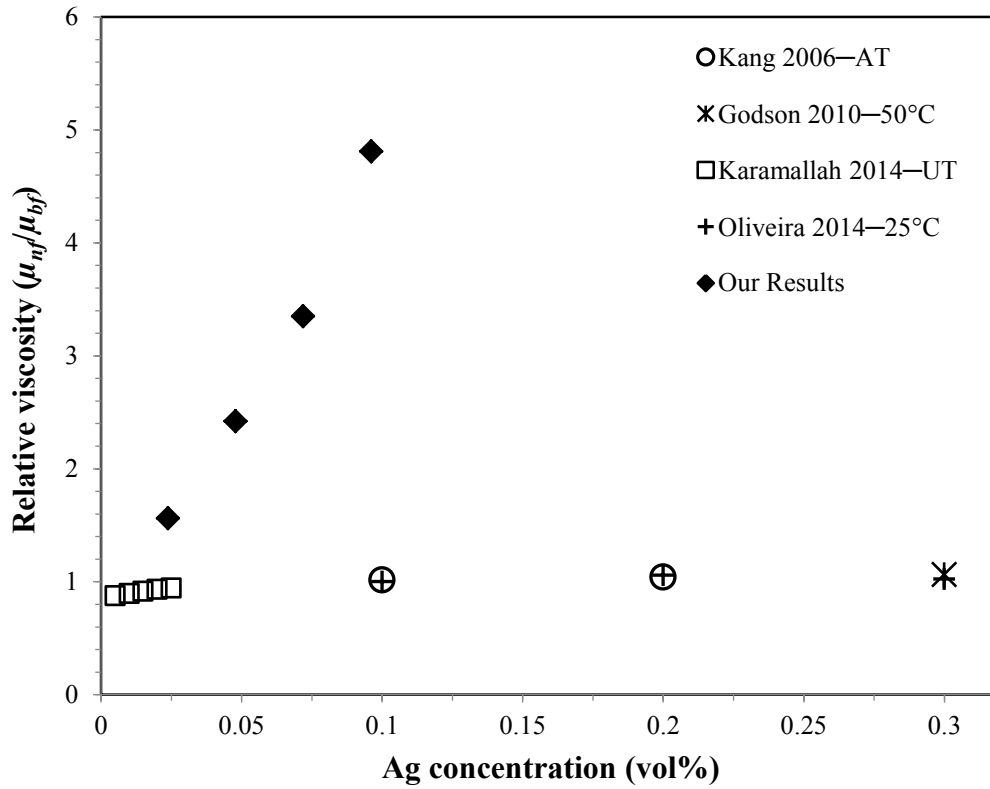


Figure 3.9 Relative viscosity with different Ag nanoparticle concentrations (vol%) compared by Godson et al. (2010), Kang et al. (2006), Karamallah & Sultan 2014 and Oliveria et al. (2012) (AT: ambient temperature, UT: unknown temperature)

On the other hand, Swei & Talbot (2002) concluded that the viscosity of aqueous PVP solutions increases considerably with increasing particle concentration from 2 to 3 wt% for  $K$ -values ranging from 92.1 to 95.4. PVP of molecular weights ranging from 2500 to 3000000 can be generally classified according to the  $K$  value, known as Fikentscher's viscosity coefficient, which is assigned to various grades of PVP present a function of the degree of polymerization, the average molecular weight and the viscosity (Fikentscher, & Mark, 1929). The  $K$ -value can be calculated by Fikentscher's formula:

$$K = \frac{\sqrt{300c \log(\mu_{rel}) + (c + 1/5c \log(\mu_{rel}))^2 + 1/5c \log - c}}{0.15c + 0.003c^2} \quad (3.2)$$

Where  $\mu_{rel}$  is the relative viscosity,  $c$  is the concentration in g/100 mL in solution and  $K_0$  represents  $K/1000$ . The  $K$ -value is based on the viscosity measurements, given by the Fikentscher equation:

$$\frac{\log \mu_{rel}}{c} = \frac{75K_0^2}{1+1.5K_0^2} + K_0 \quad (3.3)$$

Since the PVP has been commonly classified as range in between 15 and 130  $K$ -value in the majority of the literature (Dahima, 2016; Kwan, Chiu, Chang, Wu, & Huang, 2011; Swei, & Talbot, 2002), Fikentscher equation has been limited to this range, as demonstrated in Figure 3.10. The comparison between the experimental data and the results of Zhou et al. (2012b) in conjunction with Fikentscher equation shows that, our sample show a similar trend with higher  $K$ -values (Figure 3.10). Therefore, it looks reasonable to infer that PVP has a strong influence on Ag nanoparticles because of its leading effect.

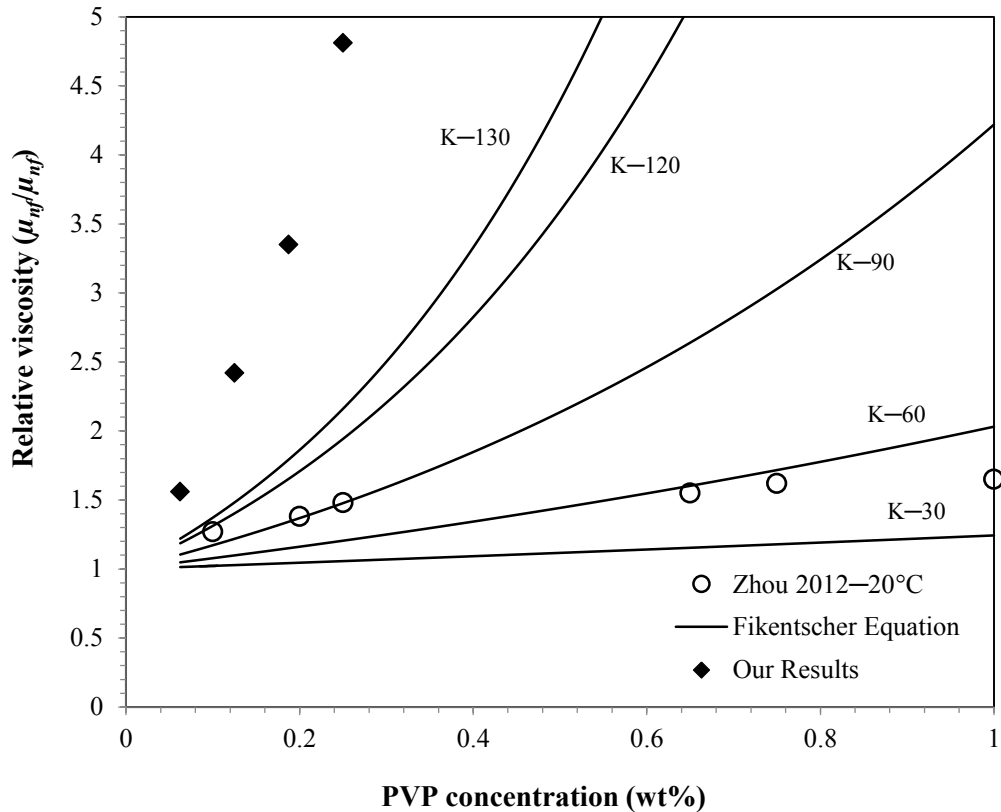


Figure 3.10 Variation of relative viscosity with different PVP concentrations (wt%) compared by Fikentscher equation and experimental results of Zhou et al. (2012b) (AT: ambient temperature)

In consideration of our experimental results, the  $K$ -value of our samples, calculated from Eq. (3.1), is equal to K-198, K-199, K-191 and K-190 for 0.0625, 0.125, 0.1875 and 0.25 wt% concentration of PVP, respectively. However, these  $K$  values are higher than the ones considered in literature. As mentioned by Sharma & Jain (2011), the aqueous PVP solution becomes poorer with increase in chain length and a further disadvantage of PVP with high molecular weight is their much higher viscosity. Based on this consideration, high relative viscosity of our samples is likely to be associated with the average molecular weight of PVP and surely also with Ag nanoparticles.

### 3.3 Thermal Performance of Ag–water Nanofluids in SPNCmL

The temperature is the only measurable data due to the fact that the mini loop is a reduced dimensional system. For this reason,  $\Delta T_{heater}$  as the average temperature difference of the fluid between outlet ( $T_2$ ) and inlet ( $T_5$ ) of the heater side was defined to determine the thermal stability of system (Turgut, & Doğanay, 2014).  $\Delta T_{heater}$  parameter also represents the amount of the heat removed from the system.

$$\Delta T_{heater} = T_2 - T_5 \quad (3.4)$$

The system stability is denoted by the steady-state curves which are given by the variation of  $\Delta T_{heater}$  and  $T_{max}$  versus time. It is clearly seen from Figure 3.11 and Figure 3.12, the thermal stability of mini loop shows same behavior for both water and 0.25% Ag–water nanofluid at all applied power. Moreover, the quiescent state time reduces with decreasing power and inclination angle. When the loop reaches the steady-state conditions, it is observed that the fluid always circulates in a counter-clockwise direction. The reason of this motion is possibly the lack of a symmetrical geometric manufacturing of the mini loop.

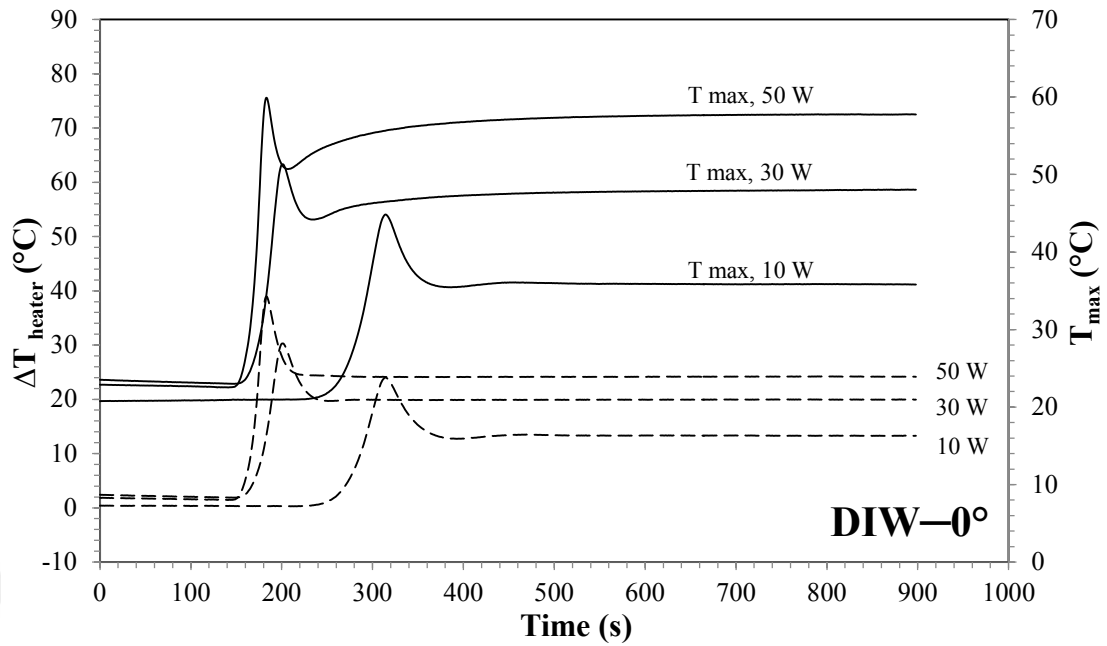


Figure 3.11 Time dependent variation of  $\Delta T_{\text{heater}}$  and  $T_{\text{max}}$  at  $0^\circ$  inclination angle for DIW

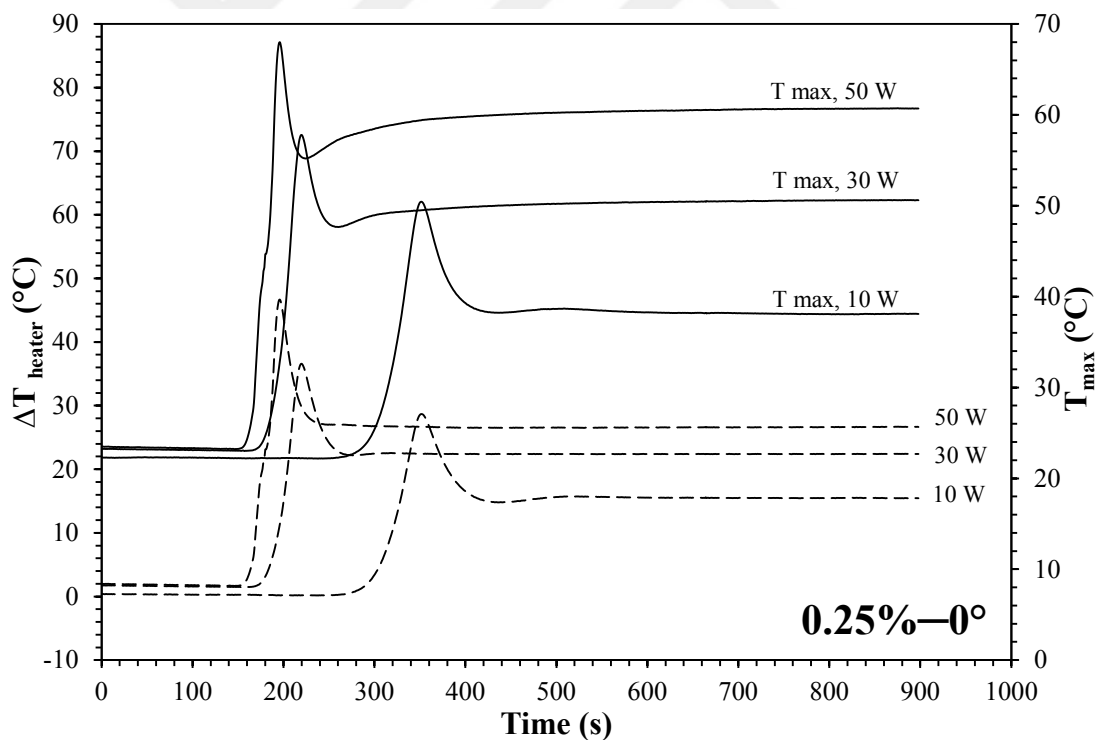


Figure 3.12 Time dependent variation of  $\Delta T_{\text{heater}}$  and  $T_{\text{max}}$  at  $0^\circ$  inclination angle for 0.25 wt% Ag-water nanofluid

Thermal stability of the mini loop for  $30^\circ$  and  $60^\circ$  inclination angles shows similar behavior as  $0^\circ$  inclination angle. Figure 3.13 demonstrated that the quiescent state time increases with increase in inclination angle.

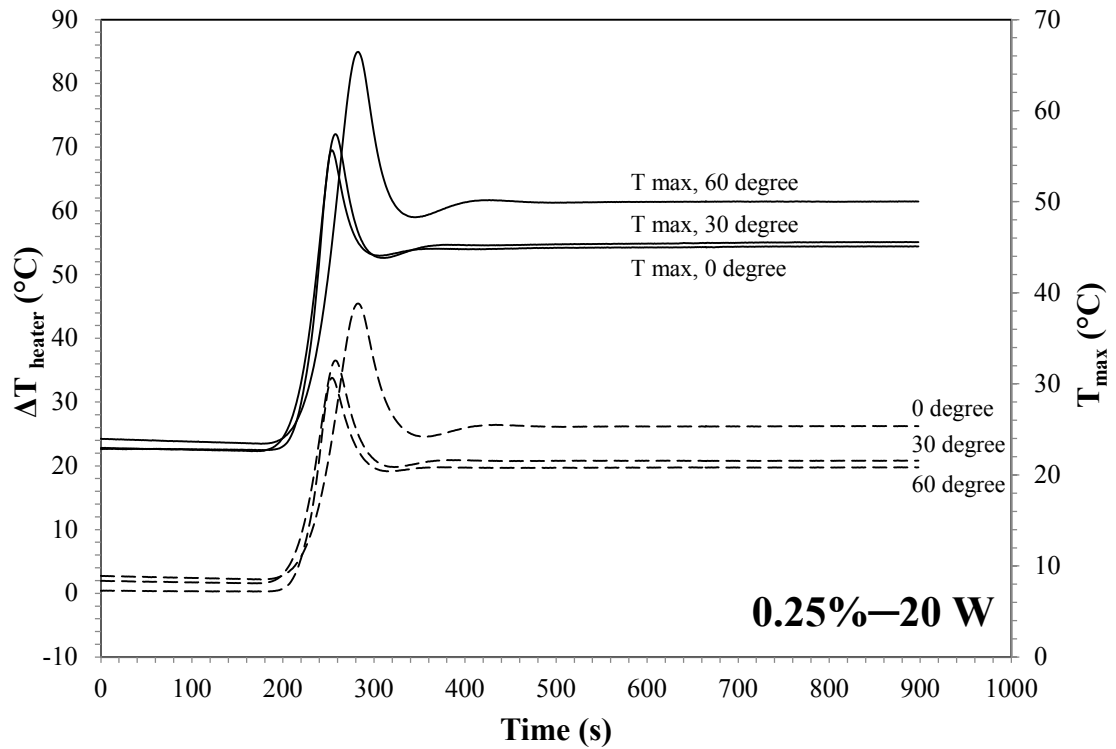


Figure 3.13 Time dependent variation of  $\Delta T_{\text{heater}}$  and  $T_{\text{max}}$  of 0.25 wt% Ag–water nanofluid for different inclination angle at 20 W

Haddad, Oztop, Nada & Mataoui (2012) reviewed the effect of nanofluids for both single- and two-phase models on natural convective heat transfer systems. They reported that most of the numerical results show that the presence of nanofluid enhances the heat transfer capability, whereas experimental results show that nanofluids deteriorate the heat transfer. Taylor et al. (2013) demonstrated that the obtained results need to be properly non-dimensionalized, since it is difficult to draw a conclusion only by considering the heat transfer coefficient. Therefore, an effectiveness factor as a non-dimensional parameter was utilized to specify the thermal performance of fluid in the SPNCmL. Since the only measurable data is temperature, the effectiveness factor which represents the ratio of actual to maximum possible heat transfer through the system (Doğanay and Turgut 2015).

$$\varepsilon = \frac{T_2 - T_5}{T_2 - T_6} \quad (3.5)$$

Based on the calibrated temperature measurements, the maximum uncertainty of the effectiveness factor was estimated to be 1.5%. The uncertainty bars is not shown in Figures in order to avoid unclarity in the graphs, which will confuse the readers. Figure 3.14 depicts the effect of concentration on the effectiveness of mini loop as a function of power. It is clearly seen that the effectiveness of the system increases with increasing nanofluid concentration. This result is valid for the all supplied powers. The effectiveness also shows a decrement with the increase in power because of the fixed temperature of the cooling bath which causes increase in the maximum possible heat transfer.

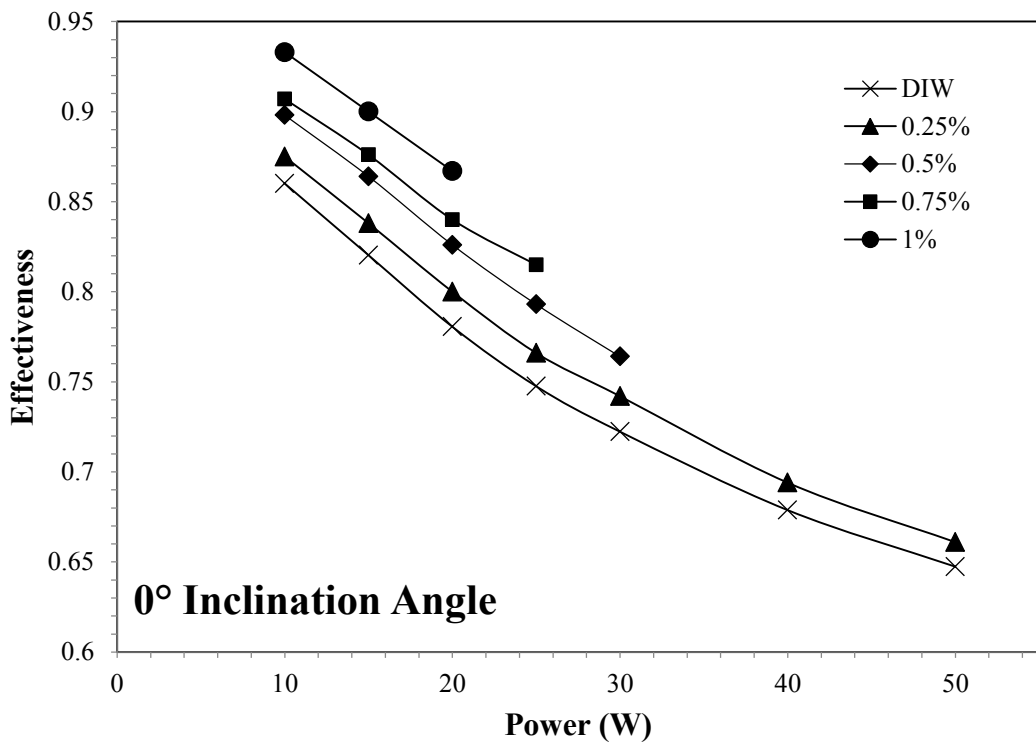


Figure 3.14 Effectiveness variation as a function of power for DIW and Ag nanofluid with different concentration (wt%)

As seen in Figure 3.15 the effect of inclination angle was investigated at 0°, 30° and 60° by comparison between 0.25% Ag–water nanofluid and base fluid. It is indicated that the effectiveness of both samples show a significant enhancement with increasing inclination angle.

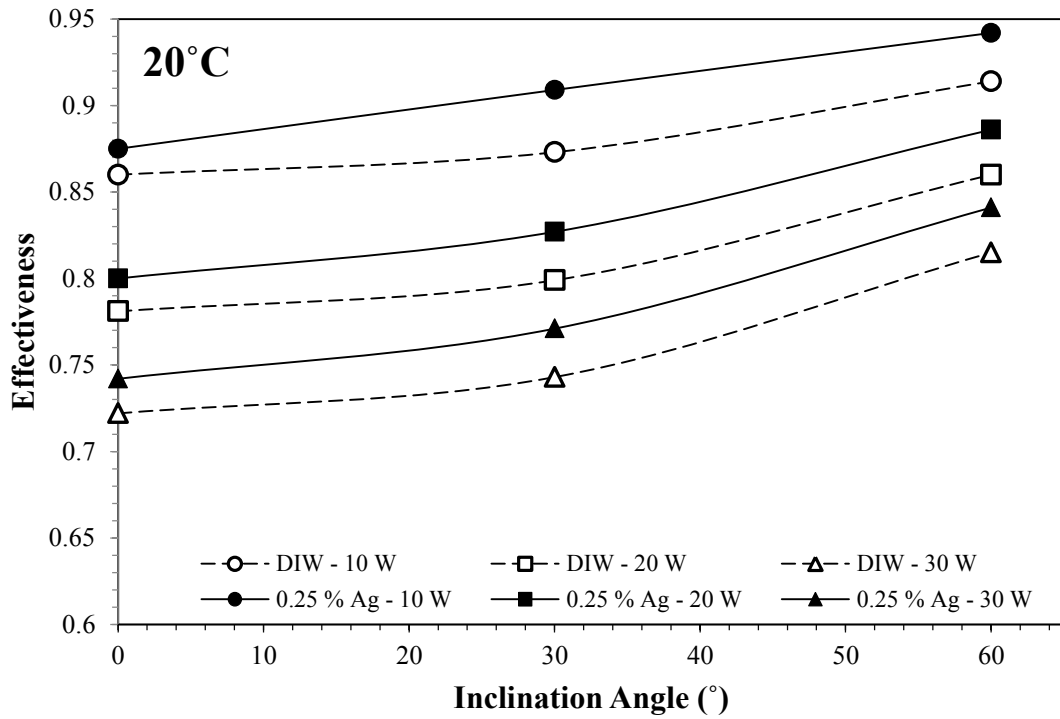


Figure 3.15 Effectiveness variation for DIW and Ag nanofluid of 0.25 wt% concentration with different inclination angle

Since the temperature of the fluid exceeds its evaporation temperature and then becomes the water-vapor two-phase flow, power range of tested nanofluid diminished at higher particle concentration. Although the 0.25% Ag–water nanofluid can be measured till 50 W, measurement of sample with 1 wt% concentration scarcely reached up to 20 W. In order to explain these results one must consider the hydrodynamic behavior of nanofluid into account. The steady state mass flow rate and velocity of the samples could not be measured due to the fact that the mini loop has reduced dimensions. For this reason the fluid velocity was calculated from Eq. (3.6) and Eq. (3.7), derived by Vijayan, Nayak, Pilkhwal, Saha, & Raj (1992) and used for nanofluids by Doğanay & Turgut (2015), Nayak et al. (2008) and Nayak et al. (2009)

$$\dot{m}_{ss} = \left[ \frac{2 g \Delta \rho H P D^b A^{2-b} \rho_{bf}}{p \Delta T \mu_r^b N_G C_e} \right]^{\frac{1}{3-b}} \quad (3.6)$$

$$V_{ss} = \frac{\dot{m}_{ss}}{A} \quad (3.7)$$

Where  $\dot{m}_{ss}$  is the steady state flow rate,  $P$  is the applied power at heater,  $g$  is the gravitational acceleration,  $\Delta\rho$  is the average density difference between outlet and inlet of heater.  $H$  is the height of the loop,  $D$  is the hydraulic diameter,  $A$  is the cross sectional area of the pipes,  $\rho_{bf}$  is the base fluid density,  $\Delta T$  is the average temperature difference between outlet and inlet of heater,  $\mu_r$  is the reference viscosity which measured by Brookfield Viscometer,  $C_e$  is the effective specific heat which estimated by Eq. (3.8), and  $p$  and  $b$  are constants of friction factor as  $f=p/Re^b$ . The density was adopted from Table 2.1.  $N_G$  is defined by Vijayan et al. (1992) which represents the effective loss coefficient of the entire loop (Eq. 3.9).

$$C_e = \frac{\phi_{np}(\rho C)_{np} + (1-\phi_{np})(\rho C)_{bf}}{\phi_{np}\rho_{np} + (1-\phi_{np})\rho_{bf}} \quad (3.8)$$

$$N_G = \frac{L_t}{D_r} \sum_{i=1}^N \left( \frac{l_{eff}}{d^{1+b} a^{2-b}} \right)_i \quad (3.9)$$

where  $l$ ,  $a$  and  $d$  are non-dimensional parameters, respectively  $l_i=L_i/L_b$ ,  $a_i=A_i/A_r$ , and  $d_i=D_i/D_r$ .

The velocity of fluids in SPNCmL is affected by the variation of gravity for different angles than  $0^\circ$  (Doğanay, & Turgut, 2015). For this reason the Eq. (3.6) should be corrected with  $g_{cor}=g\cos\theta$ , as it seen in Eq. (3.10).  $\theta$  is the inclination angle of the SPNCmL.

$$\dot{m}_{ss} = \left[ \frac{2 g \cos \theta \Delta \rho H P D^b A^{2-b} \rho_{bf}}{p \Delta T \mu_r^b N_G C_e} \right]^{\frac{1}{3-b}} \quad (3.10)$$

The steady state flow rate determined according to Eq. (3.6) and Eq. (3.10) for the system with  $0^\circ$  and greater than  $0^\circ$  inclination angles, respectively. Figure 3.16 and Figure 3.17 indicate the steady state velocity of Ag—water nanofluids as a function of input power. It is clearly seen from Figure 3.16 that, the steady state velocity of the nanofluid sample decreases with the increase in the concentration, which is probably owing to the effect of viscosity increase. It is also indicated that the

nanofluid velocity shows a decrement with increasing inclination angle because of the effect of gravitational acceleration, as shown in Figure 3.17. Additionally, the increase in the applied power causes increase of the fluid velocity which affected by the density gradients between hot and cold sections.

Since the velocity decreases, fluid spends more time at heater side and exposes more heat extraction. In the case of high heat extraction, the evolution of two-phase flow mentioned above is possible. This means that the system is more convenient for low power inputs or concentrations.

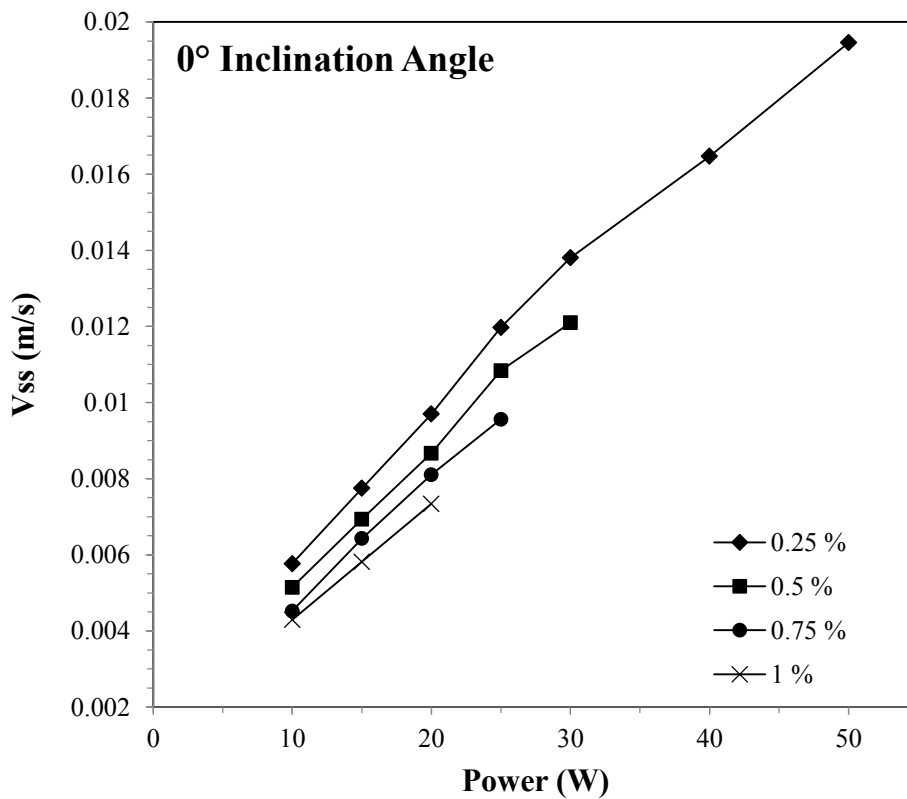


Figure 3.16 Steady state velocity in the SPNCmL versus input power for 0° inclination angle

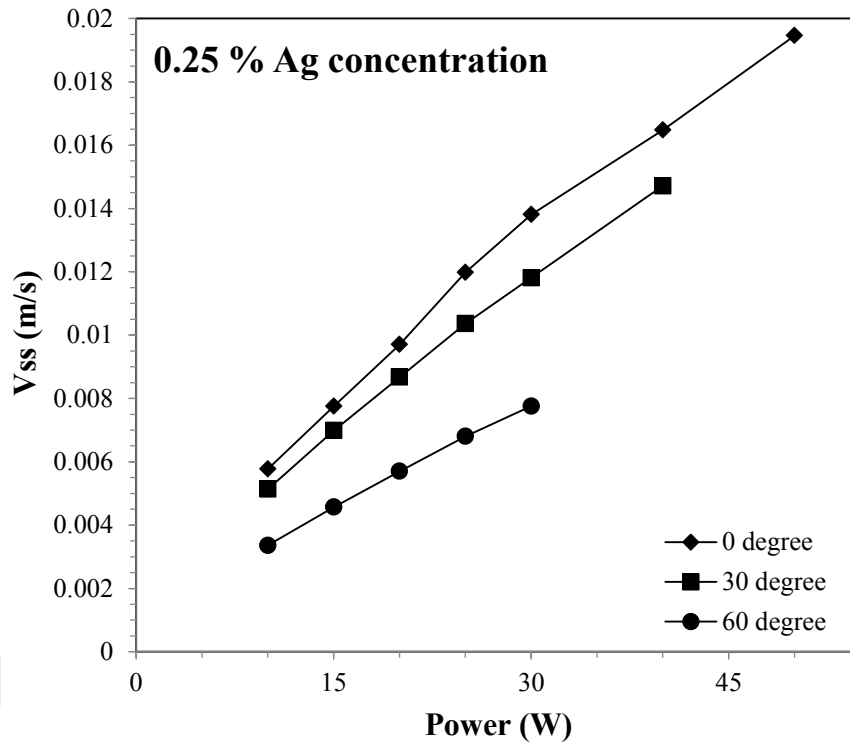


Figure 3.17 Steady state velocity in the SPNCmL versus input power for 0.25 wt% Ag concentration

In order to achieve better precision for the thermal performance of Ag–water nanofluid in more detail, our experimental results were compared with the data of Doğanay & Turgut (2015) which includes Al<sub>2</sub>O<sub>3</sub>–water nanofluid in the same system. Comparison of the effectiveness of the system working with Ag and Al<sub>2</sub>O<sub>3</sub> nanofluids at 0° inclination angle demonstrated in Figure 3.18. To obtain a clear solution, effectiveness values of nanofluids were normalized with de-ionized water. The effectiveness of Ag–water nanofluid shows an enhancement with increase in the particle concentration, which were in agreement with the effectiveness of Al<sub>2</sub>O<sub>3</sub>–water nanofluid (Doganay, & Turgut, 2015). It is also found that some apparent contradictions between both nanofluids are obtained by applying various powers. Although Al<sub>2</sub>O<sub>3</sub>–water nanofluid has an almost constant effectiveness ratio with respect to applied power, there is a significant enhancement for Ag–water nanofluid, especially for higher concentration.

Table 3.1 involves specifications of our study and study of Doganay & Turgut (2015) such as; base fluid and nanoparticle type, particle size, particle concentration, surfactant type and range of effectiveness ratio. In order to understand these complex transport phenomena, it is important to underline the role of relation between surfactant and nanoparticle. Doğanay & Turgut (2015) utilized the acetic acid (0.1–0.3% by wt) as a surfactant for the stability of Al<sub>2</sub>O<sub>3</sub>-water nanofluid. Xia et al. (2014) concluded that the thermal conductivity ratio of Al<sub>2</sub>O<sub>3</sub>-water nanofluid decreases with the increase of PVP concentration. However, acetic acid does not have a significant impact on thermal conductivity in contradistinction to PVP (Bleazard, Sun, & Teja, 1996). Based on this approach, nanofluid containing PVP surfactant should be examined more intensively and carefully because of the fact that the particle concentration of PVP (relative to Ag) plays an important role in determining the thermal performance of nanofluid.

Table 3.1 Summary of information of Doğanay & Turgut (2015) and current experimental investigations on viscosity

Article	Particle-base fluid	Surfactant	Particle wt% concentration	Particle size (nm)	Range of effectiveness ratio ( $\epsilon_{nf}/\epsilon_{bf}$ )
Doğanay & Turgut 2015	Al <sub>2</sub> O <sub>3</sub> -water	Acetic Acid	3.6–10	10 and 30	1.006–1.073
Current Study	Ag-water	PVP	0.25–1	15	1.017–1.111

The reason of this contradiction is not only the concentration of PVP in nanofluid, but also the temperature effect on PVP. As mentioned above, PVP shows a barrier effect on Ag nanoparticles. With increasing temperature, PVP loses this influence due to the loss of polymer binding (Singh, & Raykar, 2008) and then Ag nanoparticle leads to reveal its heat transfer potential. Therefore, the effectiveness ratio of water based Ag nanoparticles freed from PVP binding shows a better enhancement with the increase in the applied power. However, this enhancement cannot come through for the low concentrations, as seen in Figure 3.18. This relation is also justified by the viscosity-temperature relationship. Although the nanofluids with low concentrations have an almost constant relative viscosity and thermal performance with increasing

temperature and applied power, respectively, there are more noticeable variations for higher concentration. It is also resulted from Figure 3.18 that the effectiveness ratio of 1 wt% Ag—water nanofluid shows approximately 1.1% increase than the 10 wt% Al<sub>2</sub>O<sub>3</sub>—water nanofluid for supplied power of 10 W. Based on this consideration, it may be regarded that Ag nanoparticles are more efficient to satisfy the need of cooling systems, especially for low concentrations.

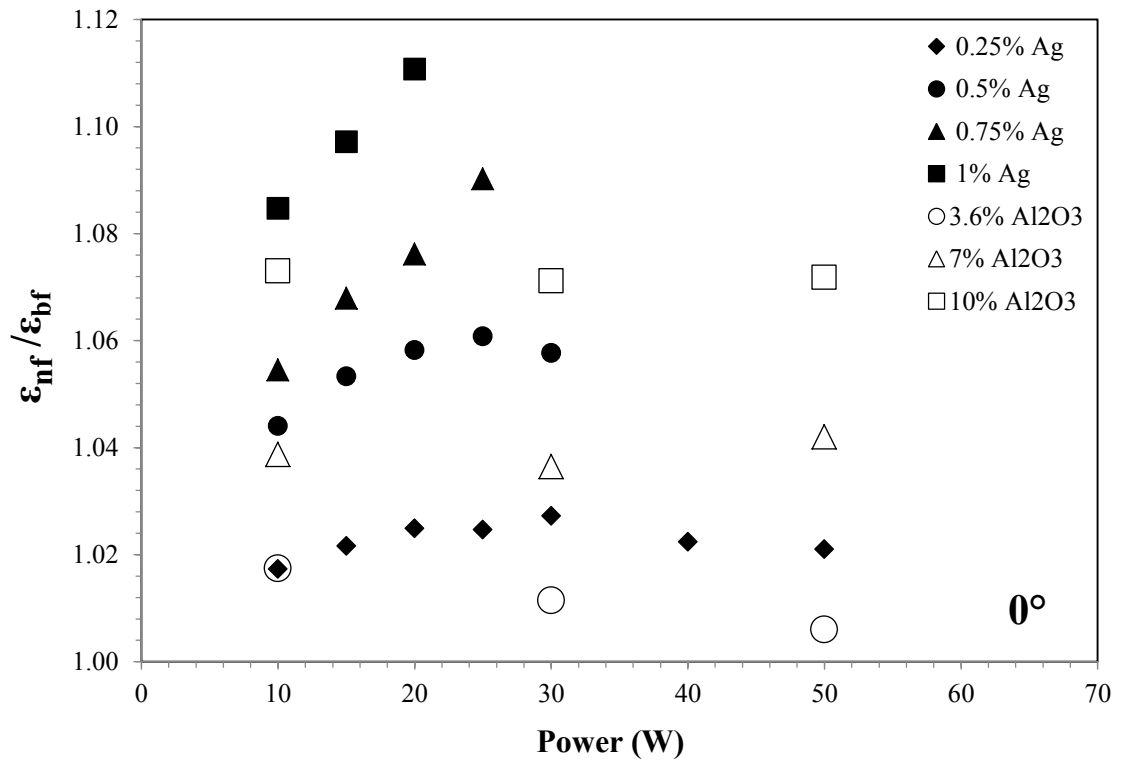


Figure 3.18 Comparison of effectiveness ratio of Ag and Al<sub>2</sub>O<sub>3</sub> nanofluid (Doğanay & Turgut, 2015) at 0° inclination angle

## CHAPTER FOUR

### CONCLUSIONS

In the present study, thermal conductivity and viscosity of Ag—water nanofluid containing PVP surfactant and its thermal performance in a SPNCmL were investigated. The important details are concluded below:

- ✓ The thermal conductivity of nanofluids decreases with the increasing concentration. The maximum deterioration of thermal conductivity is 11.5% for 1 wt%.
- ✓ The viscosity of nanofluid decreases significantly with increasing temperature and increases with increasing concentration. The maximum enhancement of viscosity is 4.81 for 1 wt% at 20 C°.
- ✓ Compared to literature, our sample was found to be more viscous and thermally less conductive. However, we determined that our thermal conductivity and viscosity results appear to be more compatible with the data of PVP solutions.
- ✓ The quiescent state time reduces as the power increases.  $\Delta T_{\text{heater}}$  and  $T_{\text{max}}$  increases with the increase of inclination angle and particle concentration.
- ✓ All the nanofluid samples show a higher effectiveness factor than the DIW and the effectiveness of the system is enhanced with increase in particle concentration and inclination angle at all applied power.
- ✓ At the same conditions, effectiveness of Ag—water nanofluids is significantly higher than the values of water based  $\text{Al}_2\text{O}_3$ —water nanofluids.

- ✓ While  $\text{Al}_2\text{O}_3$ –water nanofluids have an almost constant effectiveness ratio with respect to applied power, Ag–water nanofluids show an enhancement, especially for higher concentrations.
  
- ✓ The system is more convenient for lower power inputs or concentrations due to the evolution of two-phase flow.

According to aforementioned conclusion, it is observed that the PVP has an important effect on thermophysical properties and thermal performance of Ag–water nanofluid. The disparity between our results and the literature data is related with that the Ag nanoparticles cannot reveal its potential due to the fact that PVP has a strong barrier effect on surface of the particles. To achieve a better thermal performance and understanding of the physical phenomena between surfactant and nanoparticles, the effects of temperature on thermophysical properties and molecular weight of surfactant should be employed in future studies.

## REFERENCES

- Abdelrazek, E. M., Ragab, H. M., & Abdelaziz, M. (2013). Physical characterization of poly (vinylpyrrolidone) and gelatin blend films doped with magnesium chloride. *Plastic and Polymer Technology*, 2(1), 1-8.
- ASHRAE Handbook Fundamentals (1985). *American society of heating, refrigerating and air-conditioning engineers inc.*, Atlanta, USA.
- Barrett, T. R., Robinson, S., Flinders, K., Sergis, A., & Hardalupas, Y. (2013). Investigating the use of nanofluids to improve high heat flux cooling systems. *Fusion Engineering and Design*, 88(9), 2594-2597.
- Bandarra Filho, E. P., Mendoza, O. S. H., Beicker, C. L. L., Menezes, A., & Wen, D. (2014). Experimental investigation of a silver nanoparticle-based direct absorption solar thermal system. *Energy Conversion and Management*, 84, 261-267.
- Basu, D. N., Bhattacharyya, S., & Das, P. K. (2012). Performance comparison of rectangular and toroidal natural circulation loops under steady and transient conditions. *International Journal of Thermal Sciences*, 57, 142-151.
- Basu, D. N., Bhattacharyya, S., & Das, P. K. (2013). Influence of geometry and operating parameters on the stability response of single-phase natural circulation loop. *International Journal of Heat and Mass Transfer*, 58(1), 322-334.
- Bi, S., Guo, K., Liu, Z., & Wu, J. (2011). Performance of a domestic refrigerator using TiO<sub>2</sub>-R600a nano-refrigerant as working fluid. *Energy Conversion and Management*, 52(1), 733-737.
- Bleazard, J. G., Sun, T. F., & Teja, A. S. (1996). The thermal conductivity and viscosity of acetic acid-water mixtures. *International Journal of Thermophysics*, 17(1), 111-125.

- Bruggeman, D. A. G. (1935). Calculation of various physics constants in heterogenous substances I Dielectricity constants and conductivity of mixed bodies from isotropic substances. *Annals of Physics*, 24(7), 636-664.
- Buschmann, M. H. (2013). Nanofluids in thermosyphons and heat pipes: Overview of recent experiments and modelling approaches. *International Journal of Thermal Sciences*, 72, 1-17.
- Cahill, D. G. (1990). Thermal conductivity measurement from 30 to 750 K: the  $3\omega$  method. *Review of Scientific Instruments*, 61(2), 802-808.
- Chen, L., & Xie, H. (2010). Properties of carbon nanotube nanofluids stabilized by cationic gemini surfactant. *Thermochimica Acta*, 506(1), 62-66.
- Cho, T., Baek, I., Lee, J., & Park, S. (2005). Preparation of nanofluids containing suspended silver particles for enhancing fluid thermal conductivity of fluids. *Journal of Industrial and Engineering Chemistry*, 11(3), 400-406.
- Choi, S. U. S. (1995). Enhancing thermal conductivity of fluids with nanoparticles. *American Society of Mechanical Engineers*, 231, 99-106.
- Choi, S. U. S., Zhang, Z. G., Yu, W., Lockwood, F. E., & Grulke, E. A. (2001). Anomalous thermal conductivity enhancement in nanotube suspensions. *Applied Physics Letters*, 79(14), 2252-2254.
- Dahima, R. (2016). Comparative study of different approaches used for solubility enhancement of poorly water soluble drugs. *Panacea Journal of Pharmacy and Pharmaceutical Sciences ISSN: 2349-7025*, 4(4), 851-859.
- Dakrouy, A. Z., Osman, M. B. S., & El-Sharkawy, A. W. A. (1990). Thermal properties of aqueous solutions of polyvinylpyrrolidone in the temperature range 20–80° C. *International Journal of Thermophysics*, 11(3), 515-523.

- Das, S. K., Putra, N., Thiesen, P., & Roetzel, W. (2003). Temperature dependence of thermal conductivity enhancement for nanofluids. *Journal of Heat Transfer*, 125(4), 567-574.
- Doğanay, S., & Turgut, A. (2015). Enhanced effectiveness of nanofluid based natural circulation mini loop. *Applied Thermal Engineering*, 75, 669-676.
- Eastman, J. A., Choi, S. U. S., Li, S., Yu, W., & Thompson, L. J. (2001). Anomalously increased effective thermal conductivities of ethylene glycol-based nanofluids containing copper nanoparticles. *Applied Physics Letters*, 78(6), 718-720.
- Elçiöğlü, E. B. (2013). *Experimental and theoretical investigations on alumina–water nanofluid viscosity with statistical analysis*. PhD Thesis, Middle East Technical University.
- Fikentscher, H., & Mark, H. (1929). Ueber die Viskosität lyophiler Kolloide. *Kolloid-Zeitschrift*, 49(2), 135-148.
- Ghanbarpour, M., Nikkam, N., Khodabandeh, R., & Toprak, M. S. (2015). Thermal performance of inclined screen mesh heat pipes using silver nanofluids. *International Communications in Heat and Mass Transfer*, 67, 14-20.
- Godson, L., Raja, B., Lal, D. M., & Wongwises, S. (2010). Experimental investigation on the thermal conductivity and viscosity of silver-deionized water nanofluid. *Experimental Heat Transfer*, 23(4), 317-332.
- Godson, L., Deepak, K., Enoch, C., Jefferson, B., & Raja, B. (2014). Heat transfer characteristics of silver/water nanofluids in a shell and tube heat exchanger. *Archives of Civil and Mechanical Engineering*, 14(3), 489-496.
- Goel, A., & Rani, N. (2012). Effect of PVP, PVA and POLE surfactants on the size of iridium nanoparticles. *Open Journal of Inorganic Chemistry*, 2(03), 67.

- Haddad, Z., Oztop, H. F., Abu-Nada, E., & Mataoui, A. (2012). A review on natural convective heat transfer of nanofluids. *Renewable and Sustainable Energy Reviews*, 16(7), 5363-5378.
- Haddad, Z., Abid, C., Oztop, H. F., & Mataoui, A. (2014). A review on how the researchers prepare their nanofluids. *International Journal of Thermal Sciences*, 76, 168-189.
- Hamilton, R. L., & Crosser, O. K. (1962). Thermal conductivity of heterogeneous two-component systems. *Industrial and Engineering Chemistry Fundamentals*, 1(3), 187-191.
- Hsieh, S. S., Leu, H. Y., & Liu, H. H. (2015). Spray cooling characteristics of nanofluids for electronic power devices. *Nanoscale Research Letters*, 10(1), 1-16.
- Hwang, Y., Lee, J. K., Lee, J. K., Jeong, Y. M., Cheong, S. I., Ahn, Y. C., et al. (2008). Production and dispersion stability of nanoparticles in nanofluids. *Powder Technology*, 186(2), 145-153.
- Ijam, A., & Saidur, R. (2012). Nanofluid as a coolant for electronic devices (cooling of electronic devices). *Applied Thermal Engineering*, 32, 76-82.
- Iyahraja, S., & Rajadurai, J. S. (2015). Study of thermal conductivity enhancement of aqueous suspensions containing silver nanoparticles. *AIP Advances*, 5(5), 057103.
- Jang, S. P., & Choi, S. U. (2006). Cooling performance of a microchannel heat sink with nanofluids. *Applied Thermal Engineering*, 26(17), 2457-2463.
- Kang, H. U., Kim, S. H., & Oh, J. M. (2006). Estimation of thermal conductivity of nanofluid using experimental effective particle volume. *Experimental Heat Transfer*, 19(3), 181-191.

- Karamallah, D. A. A., & Sultan, D. K. F. (2014). Experimental investigation of heat transfer enhancement and flow with Ag, TiO<sub>2</sub> ethylene glycol distilled water nanofluid in horizontal tube. *Engineering and Technology Journal*, 32.
- Karthikeyan, V. K., Ramachandran, K., Pillai, B. C., & Solomon, A. B. (2014). Effect of nanofluids on thermal performance of closed loop pulsating heat pipe. *Experimental Thermal and Fluid Science*, 54, 171-178.
- Kleinstreuer, C., & Feng, Y. (2011). Experimental and theoretical studies of nanofluid thermal conductivity enhancement: a review. *Nanoscale Research Letters*, 6(1), 1-13.
- Kwan, C. C., Chiu, W. H., Chang, N. F., Wu, P. S., & Huang, K. F. (2011). Effect of taurate surfactant and polyvinylpyrrolidone on kaolinite suspension. *Colloids and Surfaces A: Physicochemical and Engineering Aspects*, 377(1), 175-181.
- Li, D., Hong, B., Fang, W., Guo, Y., & Lin, R. (2010). Preparation of well-dispersed silver nanoparticles for oil-based nanofluids. *Industrial & Engineering Chemistry Research*, 49(4), 1697-1702.
- Lee, S., Choi, S. S., Li, S. A., & Eastman, J. A. (1999). Measuring thermal conductivity of fluids containing oxide nanoparticles. *Journal of Heat Transfer*, 121(2), 280-289.
- Madhesh, D., & Kalaiselvam, S. (2014). Experimental study on the heat transfer and flow properties of Ag–ethylene glycol nanofluid as a coolant. *Heat and Mass Transfer*, 50(11), 1597-1607.
- Mahbubul, I. M., Saidur, R., & Amalina, M. A. (2012). Latest developments on the viscosity of nanofluids. *International Journal of Heat and Mass Transfer*, 55(4), 874-885.

- Mahbubul, I. M., Saidur, R., & Amalina, M. A. (2013). Thermal conductivity, viscosity and density of R141b refrigerant based nanofluid. *Procedia Engineering*, 56, 310-315.
- Mahbubul, I. M., Chong, T. H., Khaleduzzaman, S. S., Shahrul, I. M., Saidur, R., Long, B. D., & et al. (2014). Effect of ultrasonication duration on colloidal structure and viscosity of alumina–water nanofluid. *Industrial & Engineering Chemistry Research*, 53(16), 6677-6684.
- Masuda, H., Ebata, A., & Teramae, K. (1993). Alteration of thermal conductivity and viscosity of liquid by dispersing ultra-fine particles. Dispersion of Al<sub>2</sub>O<sub>3</sub>, SiO<sub>2</sub> and TiO<sub>2</sub> ultra-fine particles. *Netsu Bussei*, 4, 226-233.
- Maxwell, J. C. (1881). A treatise on electricity and magnetism. *Clarendon Press*, 1.
- Misale, M., Devia, F., & Garibaldi, P. (2012). Experiments with Al<sub>2</sub>O<sub>3</sub> nanofluid in a single-phase natural circulation mini-loop: Preliminary results. *Applied Thermal Engineering*, 40, 64-70.
- Murshed, S. M. S., Leong, K. C., & Yang, C. (2005). Enhanced thermal conductivity of TiO<sub>2</sub>—water based nanofluids. *International Journal of Thermal Sciences*, 44(4), 367-373.
- Murshed, S. M. S., Leong, K. C., & Yang, C. (2008). Thermophysical and electrokinetic properties of nanofluids—a critical review. *Applied Thermal Engineering*, 28(17), 2109-2125.
- Murshed, S. M. S., & de Castro, C. N. (2014). Superior thermal features of carbon nanotubes-based nanofluids—A review. *Renewable and Sustainable Energy Reviews*, 37, 155-167.

- Naphon, P., & Wiriyasart, S. (2009). Liquid cooling in the mini-rectangular fin heat sink with and without thermoelectric for CPU. *International Communications in Heat and Mass Transfer*, 36(2), 166-171.
- Nayak, A. K., Gartia, M. R., & Vijayan, P. K. (2008). An experimental investigation of single-phase natural circulation behavior in a rectangular loop with Al<sub>2</sub>O<sub>3</sub> nanofluids. *Experimental Thermal and Fluid Science*, 33(1), 184-189.
- Nayak, A. K., Gartia, M. R., & Vijayan, P. K. (2009). Nanofluids: A novel promising flow stabilizer in natural circulation systems. *AIChE Journal*, 55(1), 268-274.
- Oliveira, G. A., Bandarra Filho, E. P., & Wen, D. (2014). Synthesis and characterization of silver/water nanofluids. *High Temperatures-High Pressures*, 43(1), 69-83.
- Parametthanuwat, T., Bhuwakietkumjohn, N., Rittidech, S., & Ding, Y. (2015). Experimental investigation on thermal properties of silver nanofluids. *International Journal of Heat and Fluid Flow*, 56, 80-90.
- Patel, H. E., Das, S. K., Sundararajan, T., Nair, A. S., George, B., & Pradeep, T. (2003). Thermal conductivities of naked and monolayer protected metal nanoparticle based nanofluids: Manifestation of anomalous enhancement and chemical effects. *Applied Physics Letters*, 83(14), 2931-2933.
- Paul, G., Sarkar, S., Pal, T., Das, P. K., & Manna, I. (2012). Concentration and size dependence of nano-silver dispersed water based nanofluids. *Journal of Colloid and Interface Science*, 371(1), 20-27.
- Phuoc, T. X., Soong, Y., & Chyu, M. K. (2007). Synthesis of Ag-deionized water nanofluids using multi-beam laser ablation in liquids. *Optics and Lasers in Engineering*, 45(12), 1099-1106.

- Said, Z., Saidur, R., Sabiha, M. A., Hepbasli, A., & Rahim, N. A. (2016). Energy and exergy efficiency of a flat plate solar collector using pH treated  $\text{Al}_2\text{O}_3$  nanofluid. *Journal of Cleaner Production*, *112*, 3915-3926.
- Saidur, R., Kazi, S. N., Hossain, M. S., Rahman, M. M., & Mohammed, H. A. (2011). A review on the performance of nanoparticles suspended with refrigerants and lubricating oils in refrigeration systems. *Renewable and Sustainable Energy Reviews*, *15*(1), 310-323.
- Salehi, J. M., Heyhat, M. M., & Rajabpour, A. (2013). Enhancement of thermal conductivity of silver nanofluid synthesized by a one-step method with the effect of polyvinylpyrrolidone on thermal behavior. *Applied Physics Letters*, *102*(23), 231907.
- Sharma, P., Baek, I. H., Cho, T., Park, S., & Lee, K. B. (2011). Enhancement of thermal conductivity of ethylene glycol based silver nanofluids. *Powder Technology*, *208*(1), 7-19.
- Sharma, A., & Jain, C. P. (2011). Solid dispersion: A promising technique to enhance solubility of poorly water soluble drug. *International Journal of Drug Delivery*, *3*(2), 149.
- Singh, A. K., & Raykar, V. S. (2008). Microwave synthesis of silver nanofluids with polyvinylpyrrolidone (PVP) and their transport properties. *Colloid and Polymer Science*, *286*(14-15), 1667-1673.
- Sundar, L. S., Sharma, K. V., Naik, M. T., & Singh, M. K. (2013). Empirical and theoretical correlations on viscosity of nanofluids: a review. *Renewable And Sustainable Energy Reviews*, *25*, 670-686.
- Swei, J., & Talbot, J. B. (2003). Viscosity correlation for aqueous polyvinylpyrrolidone (PVP) solutions. *Journal of Applied Polymer Science*, *90*(4), 1153-1155.

- Tavman, I., & Turgut, A. (2010). An investigation on thermal conductivity and viscosity of water based nanofluids. *Microfluidics Based Microsystems* (139-162). Netherlands: Springer.
- Taylor, R., Coulombe, S., Otanicar, T., Phelan, P., Gunawan, A., Lv, W., & et al. (2013). Small particles, big impacts: a review of the diverse applications of nanofluids. *Journal of Applied Physics*, 113(1), 011301.
- Timofeeva, E. V., Routbort, J. L., & Singh, D. (2009). Particle shape effects on thermophysical properties of alumina nanofluids. *Journal of Applied Physics*, 106(1), 014304.
- Timofeeva, E. V., Singh, D., Yu, W., & France, D. (2013). Engineered nanofluids for heat transfer and novel applications. *NSTI-Nanotech*, 2, 404-407.
- Turgut, A., Sauter, C., Chirtoc, M., Henry, J. F., Tavman, S., Tavman, I., & et al. (2008). AC hot wire measurement of thermophysical properties of nanofluids with  $3\omega$  method. *The European Physical Journal Special Topics*, 153(1), 349-352.
- Turgut, A., & Doğanay, S. (2014). Thermal performance of a single phase natural circulation mini loop working with nanofluid. *High Temperatures-High Pressures*, 43(4), 311-320.
- Turgut, A., Sağlanmak, Ş., & Doğanay, S. (2016). Nanoakışkanların Isıl İletkenlik ve Viskozitesinin Deneysel İncelenmesi: Tanecik Boyutu Etkisi. *Journal of the Faculty of Engineering & Architecture of Gazi University*, 31(1).
- Tyagi, H., Phelan, P., & Prasher, R. (2009). Predicted efficiency of a low-temperature nanofluid-based direct absorption solar collector. *Journal of Solar Energy Engineering*, 131(4), 041004.

- Vanaki, S. M., Ganesan, P., & Mohammed, H. A. (2016). Numerical study of convective heat transfer of nanofluids: A review. *Renewable and Sustainable Energy Reviews*, 54, 1212-1239.
- Vijayan, P. K., Nayak, A. K., Pilkhwal, D. D., Saha, D., & Raj, V. V. (1992). Effect of loop diameter on the stability of single-phase natural circulation in rectangular loops. *Proceedings of the Fifth International Topical Meeting on Reactor Thermal Hydraulics (NURETH-5)*, 261–267.
- Vijayan, P. K., Sharma, M., & Saha, D. (2007). Steady state and stability characteristics of single-phase natural circulation in a rectangular loop with different heater and cooler orientations. *Experimental Thermal and Fluid Science*, 31(8), 925-945.
- Warrier, P., & Teja, A. (2011). Effect of particle size on the thermal conductivity of nanofluids containing metallic nanoparticles. *Nanoscale Research Letters*, 6(1), 1-6.
- Xia, G., Jiang, H., Liu, R., & Zhai, Y. (2014). Effects of surfactant on the stability and thermal conductivity of Al<sub>2</sub>O<sub>3</sub>/de-ionized water nanofluids. *International Journal of Thermal Sciences*, 84, 118-124.
- Yu, W., Xie, H., Chen, L., & Li, Y. (2010). Investigation on the thermal transport properties of ethylene glycol-based nanofluids containing copper nanoparticles. *Powder Technology*, 197(3), 218-221.
- Zhang, Z., Zhao, B., & Hu, L. (1996). PVP protective mechanism of ultrafine silver powder synthesized by chemical reduction processes. *Journal of Solid State Chemistry*, 121(1), 105-110.
- Zhou, M., Xia, G., Chai, L., Li, J., & Zhou, L. (2012a). Analysis of flow and heat transfer characteristics of micro-pin fin heat sink using silver nanofluids. *Science China Technological Sciences*, 55(1), 155-162.

Zhou, M., Xia, G., & Chai, L. (2015). Heat transfer performance of submerged impinging jet using silver nanofluids. *Heat and Mass Transfer*, 51(2), 221-229.

Zhou, M., Xia, G., Li, J., Chai, L., & Zhou, L. (2012b). Analysis of factors influencing thermal conductivity and viscosity in different kinds of surfactant solutions. *Experimental Thermal and Fluid Science*, 36, 22-29.



## APPENDICES

### Variables

$k$	thermal conductivity (W/mK)
$T$	temperature (°C)
$K$	Fikentscher's viscosity coefficient
$\dot{m}$	mass flow rate (kg/s)
$g$	gravitational acceleration (m/s <sup>2</sup> )
$H$	height (mm)
$P$	power (W)
$D$	hydraulic diameter (mm)
$A$	cross sectional area (m <sup>2</sup> )
$V$	velocity (m/s)
$C$	specific heat (kJ/kg °C)
$L$	length (mm)
$p$	constant of $f=p/Re^b$
$N$	effective lost coefficient

### Abbreviations

EG	ethylene glycol
DIW	de-ionized water
SDBS	sodium dodecyl benzene sulfonate
PVP	polyvinylpyrrolidone
SDS	sodium dodecyl sulfate
CTAB	cetyltrimethylammonium bromide
wt	weight
vol	volume
NCL	natural circulation loop

AT	ambient temperature
SPNCL	single-phase natural circulation loop
TPNCL	two-phase natural circulation loop
SPNCmL	single-phase natural circulation mini loop

### Subscripts

$nf$	nanofluid
$bf$	base fluid
$ss$	steady state
$rel$	relative
$c$	concentration in g/100 mL
$b$	constant of $f=p/Re^b$
$cor$	corrected
$r$	reference
$e$	effective
$G$	geometry
$np$	nanoparticle

### Greek letters

$\mu$	viscosity (Pa.s)
$\rho$	density(kg/m <sup>3</sup> )
$\phi$	volume fraction
$\theta$	inclination angle (°)
$\Delta$	interval
$\varepsilon$	effectiveness
$\omega$	omega0